AN ABSTRACT OF THE THESIS OF

David George Hinks (Name) for the Doctor of Philosophy (Degree)

in Chemistry (Degree) presented on August 30, 1968 (Date)

Title: THE EFFECT OF IMPURITIES ON THE GAMMA-RAY COLORATION OF POTASSIUM CHLORIDE CRYSTALS.

Abstract approved: Redacted for Privacy

Allen B. Scott

The incorporation of europium and dysprosium in potassium chloride crystals was investigated. The crystals were prepared by the Kyropoulos method from melts containing the rare-earth chlorides. The concentration of these rare-earth ions in the crystals was determined by neutron-activation analysis. The distribution coefficient of europium and dysprosium between the molten and solid potassium chloride was found to be . 21 and 1. 3 x 10^{-4}, respectively. The molar absorptivity of europium in the KCl crystals at two wavelengths, 241 and 325 mμ, was found to be 2880 and 2750 liter $mole^{-1}$ cm^{-1}, respectively. The crystals doped with dysprosium did not exhibit any absorption bands.

The effect of europium, dysprosium, praseodymium, calcium, and lead on the gamma-ray coloration of KCl crystals was studied. It was found that these five cations had the same qualitative effect on the

coloration curve of pure KCl, although the magnitude of the effect depended on the specific impurity. At low impurity concentrations the total first-stage coloration was not significantly changed, however, the rate of second-stage coloration was suppressed. As the impurity concentration was increased further, the coloration during the first stage increased and the second-stage coloration rate began to increase after reaching a minimum. The minimum in the rate of the second-stage coloration occurred at impurity concentrations below 1×10^{16} ions per cc. After the minimum in the second-stage rate of coloration had been attained, the ratio of the total first-stage coloration to the second-stage rate of coloration was a constant which was independent of the impurity concentration.

Crystals of potassium chloride were grown from aqueous solutions employing both convection and evaporation methods. The size and the perfection of the crystals were the same for both solution-grown methods. The dislocation density of the solution-grown crystals was a factor of three less than crystals grown from the melt.

The solution-grown crystals exhibited lower first-stage coloration than the melt-grown crystals, however, in the second stage the rate of coloration was larger for the solution-grown crystals. The second stage, which was linear for the melt-grown crystals, was generally not linear for the solution-grown crystals.

The gamma-ray coloration of several nominally pure KCl

crystals obtained from several different sources was investigated. From this study it was suggested that the colorability can be employed as a criterion of purity; the pure crystals will have a small first-stage coloration and a large second-stage rate of coloration. The ratio of the total first-stage coloration to the rate of second-stage coloration will become smaller as the purity increases. However, there are differences between the purity order established by the above criterion and conductivity data.

The Effect of Impurities on the Gamma-Ray Coloration of Potassium Chloride Crystals

by

David George Hinks

A THESIS

submitted to

Oregon State University

in partial fulfillment of
the requirements for the
degree of

Doctor of Philosophy

June 1969

APPROVED:

Redacted for Privacy

Professor of Chemistry
in charge of major

Redacted for Privacy

Chairman of Department of Chemistry

Redacted for Privacy

Dean of Graduate School

Date thesis is presented August 30, 1968

Typed by Nancy Kerley for David George Hinks

ACKNOWLEDGMENT

The author wishes to thank Dr. Allen B. Scott for many helpful discussions.

Thanks are also due Jerry Krause for help in proof reading the manuscript, and Dr. W. J. Fredericks and L. Schuerman for supplying the purified potassium chloride.

Financial assistance from the Department of Health, Education and Welfare, in the form of an NDEA fellowship, was greatly appreciated.

TABLE OF CONTENTS

TABLE OF CONTENTS (continued)

TABLE OF CONTENTS (continued)

LIST OF TABLES

LIST OF FIGURES

LIST OF FIGURES (continued)

THE EFFECT OF IMPURITIES ON THE GAMMA-RAY COLORATION OF POTASSIUM CHLORIDE CRYSTALS

INTRODUCTION

Color Centers

Models of Color Centers

Color centers are formed in alkali halide crystals when electrons or holes are trapped at lattice defects. The centers usually absorb radiation in the ultraviolet, visible, or near-infrared region of the spectrum and have therefore been extensively studied using spectrophotometric methods. Some of the color centers also have an unpaired electron and these have been investigated with spin-resonance techniques. By the use of these methods the structure of several of the color centers has been determined.

The most prominent electron-trapped center is the F center, and it is formed when an electron is captured by a negative-ion vacancy. Other electron-excess centers are formed when electrons are trapped at anion-vacancy clusters. For example, the M center is composed of two adjacent negative-ion vacancies which have captured two electrons.

The V_K center is a hole trapped at two adjacent halide ions, and can be thought of as a X_2^- molecule-ion, where X denotes a halogen

atom. The H center is a hole trapped at a linear arrangement of four halide ions which are distributed over three anion-lattice sites. Two of the halide ions are situated at the center-anion site and one halide ion is present in each of the end-anion positions. The hole spends four to ten percent of its time at the end-halide ions. Chemically, this center can be thought of as an interstitial halogen atom. Figure 1 shows the centers described above.

The structures of the other hole-trapped centers are unknown and they are identified by the position of their optical absorption bands. They are called V centers and a particular center is denoted by a subscript, such as the V_1 center.

Production of Color Centers

Color centers can be introduced in an alkali halide crystal by several methods; the two most important methods are additive coloration and coloration by ionizing radiation. A crystal is additively colored by heating it in an atmosphere of an alkali metal. The alkali metal atoms add substitutionally to the crystal lattice, and an electron is lost by the metal atom and trapped by a negative-ion vacancy to form an F center. Only electron-excess centers are formed by this method.

Exposure of a crystal to ionizing radiation will also cause color-center formation. The radiation will produce electrons and

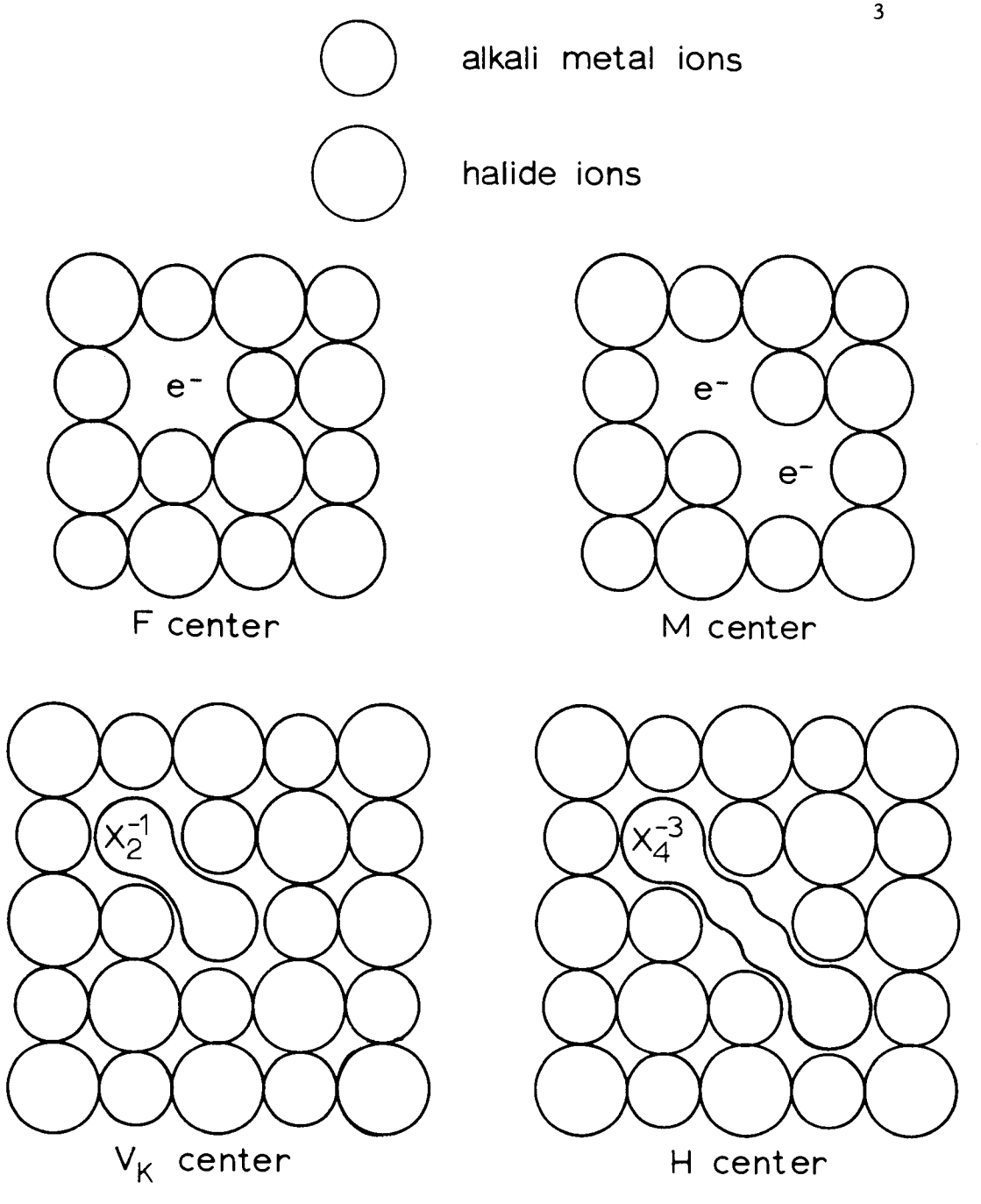

Figure 1. Color-center models. X and e^- represent halogen atoms and electrons, respectively.

holes which will be trapped to form both electron- and hole-trapped centers. Defects, such as anion vacancies and halide-ion interstitials, are also produced by the radiation. The F center is the predominant electron-trapped center produced at all temperatures; however, the temperature of the irradiation determines the hole-trapped centers which are formed.

F-Center Concentration

In KCl the F center absorbs at 560 mμ, and the concentration of F centers can be found from the area of the absorbance band. Smakula (53) derived the relationship between the concentration, N, of F centers and the area, A, of the absorption curve according to classical dispersion theory. The equation has been modified by Dexter (10) and is

$$Nf = .821 \times 10^{17} \frac{n}{(n^2+2)^2} A$$

where f is the oscillator strength of the F center and n is the index of refraction at the maximum of the F-band absorption. The units of N and A are F centers per cc and $cm^{-1}eV$, respectively.

If a Gaussian shape is assumed for the F-center absorption, the above equation becomes

$$Nf = 1.68 \times 10^{16} A_m W$$

where A_m is the absorbance per cm at the F-band maximum, W is the half-width of the F-center absorbance band in electron volts, and 1.492 has been substituted for the index of refraction at the F-band maximum in KCl. The half-width, W, is .34 eV (28) and the average of the oscillator strengths reported by several authors is .59 (54) for a Gaussian shape. Substitution of these values yields

$$N = .97 \times 10^{16} A_m$$

for the F center in KCl.

Coloration at 4° K

Color Centers Formed

The rate of F-center formation by ionizing radiation is determined by measuring the absorbance of the F band as a function of irradiation time. The concentration of F centers can then be determined from the Smakula equation. The graph of the F-center concentration versus the irradiation time or the absorbed dose is called a growth curve or a coloration curve.

At liquid-helium temperature the predominant electron-excess center produced by the radiation is the F center, although a small concentration of higher aggregate centers, such as the M center, are formed. The major hole-trapped center which is formed is the H center, however some V_K centers are also formed at this

temperature (56). Klick and Patterson (27) have also shown that many anion vacancies are produced which have not trapped electrons.

Kinetics

Rabin and Klick (41) showed that at liquid-helium temperature the rate of coloration depends only on the alkali halide, the type of radiation, and the radiation intensity. The impurity content and the dislocation density do not significantly affect the F-center growth rate. The growth curve is linear (43), although more recent results by Ritz (44) show that there is a slight downward curvature as the irradiation progresses. It requires several thousand electron volts to produce a F center at 4° K.

From the above results it appears that at liquid-helium temperature the F-center coloration is an intrinsic property of the alkali halide crystal. Any mechanism postulated for F-center production at this temperature must result in the production of Frenkel defects, that is halide-ion vacancies and interstitials, since the H center was the predominant hole-trapped center.

Mechanisms

The simultaneous production of vacancies and interstitials was first postulated by Varley (57, 58). He proposed that the halide ion is initially doubly ionized by the radiation. The resulting positive halide

ion, X^+, will be situated in an electrostatically-unfavorable environment, and a slight displacement of the lattice will cause the positive ion to be ejected from the lattice position into an interstitial position. The vacancy which results can capture an electron to form an F center, while the interstitial X^+ ion can capture an electron to form an H center.

The Varley mechanism has been criticized for several reasons. This mechanism would be expected to produce F and H centers in close proximity, but the optical measurements of Konitzer and Markham (28) and the spin-resonance work of Kaenzig and Woodruff (24) indicate that the interstitial and vacancy are several lattice spaces apart. Also, the lifetime of the X^+ ion must be long enough for the ion to be ejected from its normal site. Howard and Smoluchowski (22) found that the time for the X^+ ion to capture an electron from the conduction band was long enough for the Varley mechanism to be operative. However, Dexter (11) found that the time for the X^+ ion to capture an electron from a neighboring halide ion was not sufficient for the Varley mechanism to be operative. A recent computer simulation (6) of the Varley mechanism including the influence of lattice relaxation around the X^+ ion and assuming a sufficiently long lifetime of the positive ion indicates that the X^+ ion will not be ejected into an interstitial position.

Several modifications of the Varley mechanism have been

proposed which will lead to separated interstitials and vacancies. Howard, Vosko, and Smoluchowski (23) propose that the Cl^+ ion is formed in KCl by an Auger process. If the Cl^+ ion approaches a neighboring chloride ion to within 2.2 Å, an electron will be transferred with the formation of two chlorine atoms. Because of the large amount of energy released when the electron is transferred, the authors assume that the two chlorine atoms will not form a chlorine molecule but they will be in the antibonding state. The two chlorine atoms will then be repelled with approximately 3 eV of kinetic energy. One of the chlorine atoms may be displaced into an interstitial position by means of a series of focused collisions in the [110] direction, assuming that at each collision an electron is transferred from the chloride ion to the chlorine atom.

In order to circumvent the questions raised over the lifetime of the X^+ ion, several mechanisms have been postulated which require the single ionization of two adjacent halide ions, formed either by the single ionization of two neighboring halide ions or by the double ionization of a halide ion with the subsequent capture of an electron from an adjacent halide ion. Klick's mechanism (26), which is shown in Figure 2, requires that the two halogen atoms form a halogen molecule. The halogen molecule will fit into a vacancy and the jump of a neighboring halide ion will form a Frenkel pair. The model postulated by Williams (60) is shown in Figure 3. An induced dipole is set up on

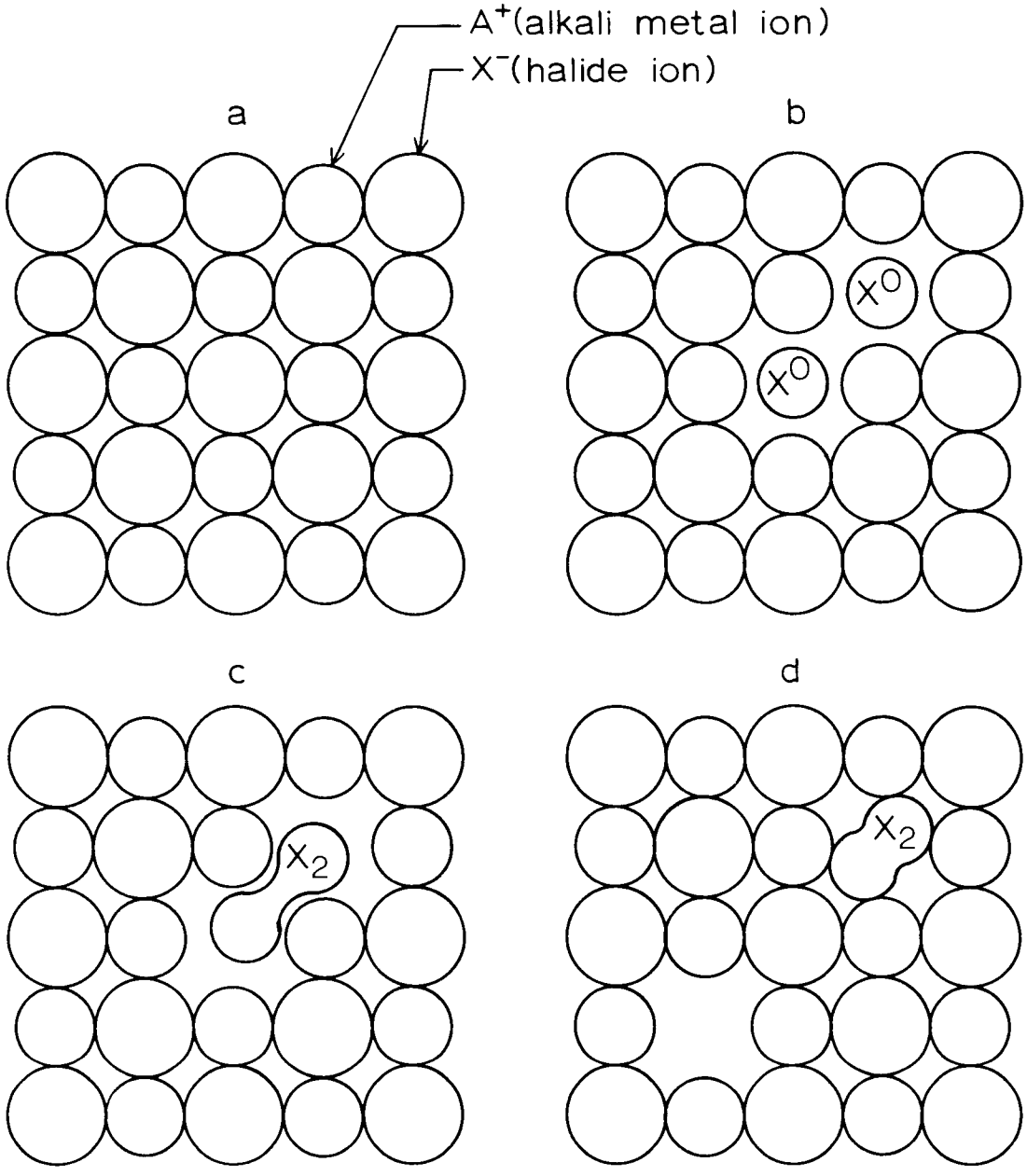

Figure 2. Klick's mechanism for F-center production.(a) crystal before irradiation, (b) formation of two adjacent halogen atoms, (c) halogen molecule formation, (d) formation of an anion vacancy by the jump of a halide ion.

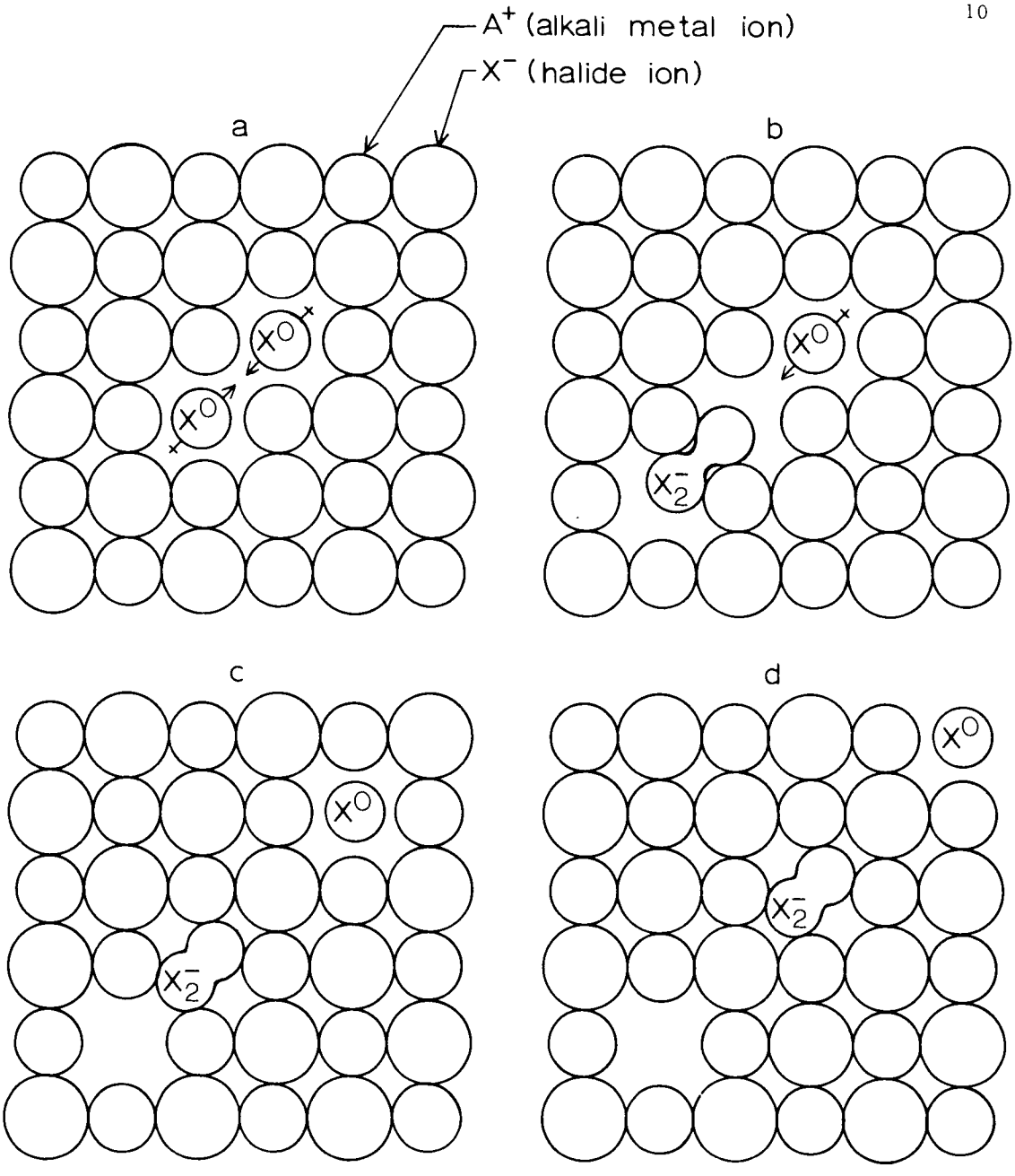

Figure 3. William's mechanism for F-center production. (a) formation of induced dipoles on the halogen atoms, (b) formation of a X_2^- molecule-ion, (c) anion-vacancy formation, (d) separation of the interstitial from the vacancy.

each halogen atom because of the noncentral Coulombic field caused by the presence of the adjacent halogen atom. Each halogen atom will then be attracted to a neighboring halide ion in the [110] direction. Some of the halogen atoms will form X_2^- molecule-ions. Because of the nonuniform field, the X_2^- ion will be attracted in the direction of the other halide ion. At this point the X_2^- ion will have gained 1.1 eV of kinetic energy. A series of "billiard ball" collisions in the [110] direction with concurrent tunneling of the hole will lead to a separation of the vacancy and the interstitial. It is assumed by Williams that the hole, which was localized on the halogen atom which did not enter into the formation of the X_2^- molecule-ion, will also migrate.

Room-Temperature Coloration

Defects Produced

As for irradiations performed at 4° K, the F center is the main electron-trapped center formed at room temperature. Since the F-center concentration formed in a crystal by the irradiation may be much larger than the initial concentration of negative-ion vacancies statistically present, it is necessary for the radiation to produce anion vacancies. However, at room temperature the structures of the hole-trapped centers are not known. This has made it difficult to

determine whether Schottky or Frenkel disorder is responsible for the negative-ion vacancy production.

The energy to form a Frenkel defect in the alkali halide lattice is large, and for this reason it had usually been assumed that interstitials were not formed at room temperature. If this is true, the process by which vacancies are produced at room temperature must be different from that at 4° K because the low-temperature mechanisms require the production of interstitials.

However, recent expansion data (9, 36) and the analysis of radiation hardening (32, 33, 51) suggest that halide interstitials are formed by irradiation at room temperature. This would allow the mechanisms postulated at 4° K to be operative at room temperature. At the present time it is not possible to say with certainty which defects are produced, therefore, the process of F-center formation is not known.

Kinetics of F-Center Formation

Unlike the irradiation at liquid-helium temperature, the rate of F-center formation at room temperature depends on the impurity content and mechanical strain in the crystal. The room-temperature coloration curve is also more complex, which led Gordon and Nowich (17) to propose that the F-center coloration could be separated into two stages. When a crystal is irradiated, there is an initial

rapid increase in the F-center concentration followed by a slow, relatively linear, increase in the F-center concentration. The initial rapid coloration is called the first-stage coloration and usually saturates between 10^{16} to 10^{17} F centers per cc for a pure crystal. The second-stage coloration is the slow coloration. At high radiation intensities the second stage may be followed by a third stage (30, 31) in which the coloration rate again becomes rapid, although still much slower than the coloration rate during the first stage. Eventually at large radiation doses the F-center concentration saturates at about 10^{18} to 10^{19} centers per cc.

During the second stage it requires several thousand electron volts to produce an F center, while an F center is produced by approximately 100 eV during the first stage. Because of the small energy necessary to produce an F center during the first stage, it is felt that the anion vacancies utilized during this stage are initially present in the crystal, probably as vacancy clusters. The second stage is thought to be due to the filling of negative-ion vacancies which are produced by the radiation.

Mitchell, Wiegand, and Smoluchowski (30, 31) have derived a five-parameter equation which fits the room-temperature coloration curve before saturation occurs. They assume that the F centers, f_i, formed from vacancies initially present in the crystal and the F centers, f_g, formed from anion vacancies produced by the irradiation

can be treated independently. Also, they postulate that the bleaching rate of the two types of F centers are different and that the rate of electron capture by the vacancies initially present and those produced by the radiation are not the same.

The total F-center concentration in the crystal is

$$f = f_i + f_g$$

The F-center concentration formed from the capture of electrons by vacancies initially present in the crystal can be determined from

$$\frac{df_i}{dt} = bn_i - \alpha f_i$$

and

$$\frac{dn_i}{dt} = \gamma \{n_o - (n_i - f_i)\} - \frac{df_i}{dt}$$

where b and α are the rate constant for electron capture by vacancies initially present in the crystal and a bleaching constant, respectively, n_i is the concentration of free negative ion vacancies, n_o is the concentration of negative ion vacancies initially present in the crystal in small clusters and γ is the rate constant for the release of anion vacancies by the clusters.

The F-center concentration generated from anion-vacancies formed by the radiation can be found from

$$\frac{df_g}{dt} = c\, n_g - \beta f_g$$

and

$$\frac{dn_g}{dt} = a - \frac{df_g}{dt}$$

where c is the rate constant for electron capture by vacancies generated by the radiation and β is a bleaching constant, a is the rate constant for the generation of anion vacancies by the radiation, and n_g is the concentration of free negative-ion vacancies.

Solving the above equations yields

$$f = n^*(1-e^{-b^*t}) + a^*t - \frac{a^*}{c^*}(1-e^{-c^*t})$$

where $n^* = \frac{bn_o}{b+\alpha}$, $a^* = \frac{c}{c+\beta}a$, $c^* = c + \beta$, and $b^* = b + \alpha$. The authors have assumed that γ, the rate constant for the release of anion vacancies from the clusters initially present in the crystal, is larger than b. If, however, γ is larger than b then $b^* = \gamma$ in the above equation.

The authors also found that a term $n_o'(1-e^{-c^*t})$ must be added to the above equation, where n is the concentration of negative-ion vacancies present nonuniformly in the crystal at dislocations. These vacancies behave as the vacancies which are generated by the radiation. It was necessary to add this term so that the equation could be fitted to the coloration curves of mechanically deformed crystals.

Rivas and Levy (45) have employed the equation

$$f = at + \sum_{i=1}^{n} A_i(1-e^{-a_i t})$$

to fit the first two stages of coloration. They found that for NaCl and KCl three exponential terms were required, although the term representing the fastest process was too small to measure accurately. This type of equation would result if the coloration was caused by a number of independent processes. An exponential term will result from each process if the defects, from which F centers are produced by a particular mechanism, undergo a first order process for the generation of the F centers. Each process may also have a linear contribution if the defects are produced linearly by the radiation.

This equation will have the same form as the equation derived by Mitchell, Wiegand, and Smoluchowski if only two exponential terms are employed. However, in this case, no physical interpretation was given to the individual parameters.

Effect of Impurities

In crystals containing divalent cation impurities, such as lead or calcium, the first-stage coloration is greatly enhanced. The effect of the impurity on the second stage has not been thoroughly investigated, although Sibley, Sonder, and Butler (52) have shown that the divalent lead impurity will suppress the very late stages of coloration.

The effect of divalent impurities on the first-stage coloration cannot be easily understood. Charge compensation requires that each

divalent ion added substitutionally to the lattice must introduce a positive-ion vacancy. Since the concentration of anion vacancies times the concentration of cation vacancies is a constant at a given temperature, an increase in the cation vacancies should decrease the concentration of anion vacancies. This should decrease the F-center coloration rate. To account for the observed increase, Crawford and Nelson (8) have proposed that a positive-ion vacancy can be converted into an anion vacancy by the irradiation. They suggest that a halide ion adjacent to the cation vacancy captures a hole, and the halogen atom which is formed relaxes into the positive-ion vacancy forming a negative-ion vacancy. The halogen atom may then form an X_2^- molecule-ion orientated along the [100] direction, although the actual defect which would be formed at room temperature is not known. Also, it should be noted that not all divalent cations affect the first-stage coloration. Rabin (40) has reported that cadmium has very little effect on the first-stage coloration.

The reason for the late-stage suppression is not thoroughly understood. Hersh (19) and Pooley (38) have suggested that F centers may be formed by radiationless recombination of electrons and holes during the later stages of coloration. The energy released by this recombination process will be sufficient to produce Frenkel defects. Pooley (39) has shown that if electron-trapping impurities are present the rate of F-center production should be reduced. This is because

electron-hole recombination occurs at the impurities without the production of F centers. Thus, the recombination rate in the lattice is reduced causing a decrease in the F-center production rate.

EXPERIMENTAL

Crystal Growth

Melt-Grown Crystals

Salt purification. Potassium chloride was purified by an ion-exchange method investigated by Fredericks, Rosztoczy, and Hatchett (14, p. 2-7). W. J. Fredericks and L. Schuerman designed and constructed the purification apparatus, and kindly supplied the purified salt. The method has been described extensively (15, p. 4-17); therefore, only a brief presentation will be given.

Reagent grade potassium chloride was dissolved in deionized water, and the resulting solution, which was 25 percent salt by weight, was filtered through Whatman's No. 1 filter paper to remove any large undissolved particles. This solution was passed through a column of Bio-Rad analytical grade Chelex 100, potassium form, followed by a bed of Dowex AG-2, chloride form. The purified solution was evaporated to dryness at 60° C in a vacuum oven employing a water aspirator. The potassium chloride was stored in polyethylene containers and throughout the purification process the salt was never in contact with glass.

Growth of crystals. Potassium chloride crystals were grown by the Kyropoulous method with the apparatus described by Holmes

(21, p. 21-39). The salt was contained in a quartz crucible in the crystal-growth apparatus. If the crystal was to contain foreign cation impurities, the reagent grade chloride of the cation was added directly to the crucible containing the potassium chloride.

The salt was heated at 300° C in a vacuum for at least 12 hours to remove any water. Then anhydrous hydrogen chloride, at one atmosphere, was placed over the salt and the furnace temperature was increased until the salt was molten. The purpose of the hydrogen chloride was to remove any hydroxides or carbonates present in the salt.

After the potassium chloride had melted, the hydrogen chloride was replaced by argon in the apparatus. Then the water cooled rod, which held a seed crystal, was lowered until the seed extended into the melt. In order to insure single-crystal formation, the furnace temperature was increased until the surface of the seed melted, then the temperature was slowly lowered until a crystal began to form. The diameter of the crystal was determined by the rate at which the seed was withdrawn from the melt. Usually, the seed-withdrawal rate was one centimeter per hour, which gave a crystal approximately one inch in diameter.

Solution-Grown Crystals

Growth by convection. Okamoto and Scott (35) have grown

potassium chloride crystals from solution using the convection method.

A saturated potassium chloride solution is contained in a polyethylene bottle, with an excess of undissolved salt present at the bottom of the bottle. A temperature gradient is maintained in the surrounding air along the length of the bottle, the bottom being hotter than the top. The solution in the lower region of the container will become warmer; and as it does so, it will dissolve some of the solid potassium chloride. Convection currents will cause this solution to raise toward the top of the bottle. Since the air surrounding the upper region of the container is cooler, heat will be lost from this solution, causing it to become supersaturated. Salt will then be deposited on a seed placed in the solution near the top of the bottle.

Figure 4 shows the apparatus employed to grow crystals from solution by convection. A rectangular enclosure 1-1/2 feet high, 2-1/2 feet long by 1 foot wide was constructed, and insulated with 1/4 inch glass wool. The base of the enclosure served as a heater, and was constructed from three pieces of 1/4 inch Transite, the center piece being wound with No. 22 Nichrome wire. A 1/2 inch plywood baffle separated the apparatus into two compartments. The baffle contained 12 holes, through which 12 250 ml ployethylene bottles were inserted. The bottles were 11 cm long by 6 cm in diameter and extended 3 cm through the baffle into the lower chamber. A cork spacer

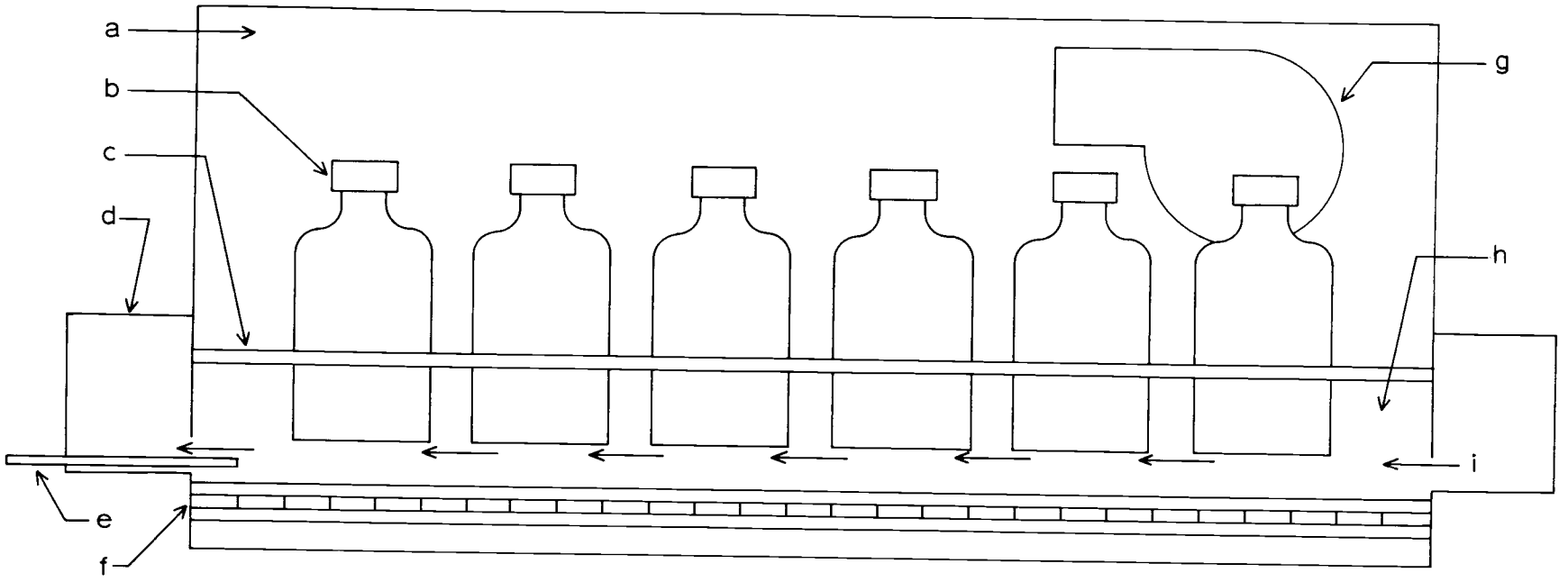

Figure 4. Apparatus for growing KCl crystals from solution by convection. (a) upper chamber, (b) 250 ml polyethylene bottles, (c) baffle, (d) external air duct, (e) control thermocouple, (f) heater, (g) blower, (h) lower chamber, (i) direction of air flow in lower chamber.

held each bottle .5 cm above the heated base.

When operating, the temperature of the lower chamber was kept at 50° C, while the upper chamber was cooler because heat was lost to the room. In order to maintain a uniform temperature in the upper chamber, air was circulated by a blower. The lower chamber was too small to incorporate a blower, but air was circulated through an external duct. A fan forced air through the lower chamber, through the insulated duct, and then back to the lower chamber.

The temperature of the lower chamber was controlled by a Yellow Springs Instrument Company Model 72 proportional controller. The sensing probe of the controller was placed at the entrance to the air duct and the control temperature was set at 50° C. Because heat was lost by the air circulating through the external air duct, the temperature in the lower chamber varied with position. Air entered from the external duct at 46.6° C and left the lower chamber at 49.6° C. The temperature of the upper chamber was 42.5° C. The temperature gradient between the upper and the lower chamber therefore depended on position, and varied from 4° at the air entrance to the lower chamber to 7° C at the air exit. The temperature variation over a period of several weeks was at most .5° C.

The saturated solutions were made from the potassium chloride purified by ion exchange. Approximately 15 grams of undissolved salt was present in each bottle. After remaining in the

apparatus for one week to insure saturation, the solutions were seeded. A nylon thread with three 1 x 1 x 3 mm seeds was placed in each bottle. The seeds were 1.5 cm apart on the thread, and the seed closest to the top of the bottle extended about .5 cm into the solution.

After two months, salt had deposited on the seeds. A single crystal was not usually produced, but each seed acted as a nucleation center for a large number of crystals. The material surrounding each seed usually contained several large single crystals of potassium chloride, the largest being about one cubic centimeter in volume. The single-crystal regions were then removed and used for the coloration experiments.

Growth by evaporation. Growth of large sodium chloride crystals by evaporation has been reported by Gruzensky (18). Crystals of potassium chloride were grown using his method. The saturated salt solution was placed in 250 ml polyethylene bottles. Several drops of deionized water were added to each bottle to give a slightly undersaturated solution, then a seed crystal was added to each solution. Six beakers were placed in each 250 mm vacuum desiccator, which contained .5 pound of phosphorus pentoxide. As the phosphorus pentoxide absorbed water, the solutions became supersaturated and salt was deposited on the seeds.

Many new seeds were formed in the bottles as the solution

evaporated. After two months, the mass of crystals at the bottom of each beaker was removed and the single-crystal regions were separated from the polycrystalline material. The crystals were approximately the same size as those obtained by the convection method.

Perfection of Solution-Grown Crystals

Inclusions. All of the solution-grown crystals contained small pockets of solution. Figure 5 shows several photographs of the crystals taken below the surface by means of an American Optical Company Model 2200 metallurgical microscope, equipped with a Model 635 35 mm photomicrographic camera.

As can be seen from Figure 5, the number and size of the inclusions vary considerably. Plates a and b show the average concentration of inclusions in the single-crystal regions while the other three plates show a higher than normal number of inclusions. The crystals employed in the coloration experiments had approximately the same number of inclusions as the crystals shown in plates a and b.

The total proportion of solution incorporated in the solution-grown crystals was not large. The crystals could be heated at 600° C without cracking or forming a powder.

Dislocations. The disolocation content of the solution-grown crystals was determined and compared to the melt-grown crystals.

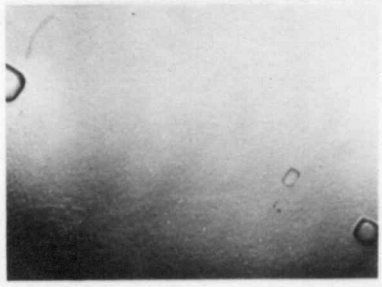

Plate a

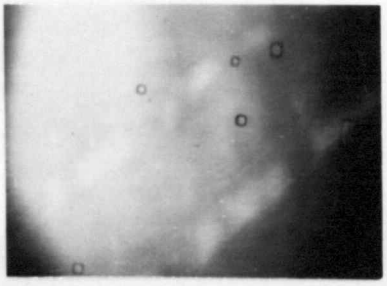

Plate b

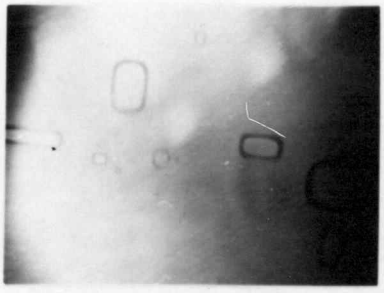

Plate c

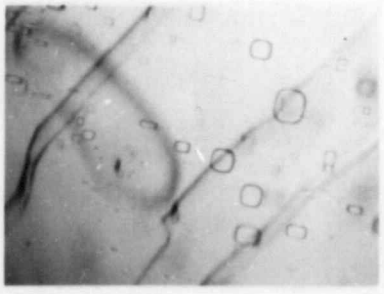

Plate d

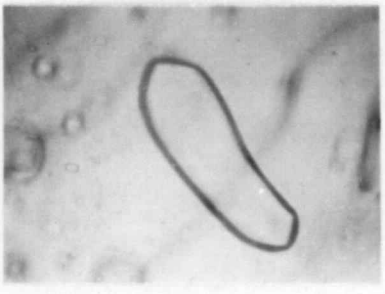

Plate e

Figure 5. Inclusions in solution-grown KCl crystals. (⟼ = 100 μ)

The etchant employed, described by Cook (7), was propionic acid containing 1.75 percent by weight of barium. The propionic acid was distilled to remove water. Barium carbonate was added to the distilled propionic acid, and the mixture was refluxed until all the barium was in solution. Etching was done by immersing the crystal in the etchant for 30 seconds, followed by a petroleum ether rinse, the petroleum ether having been dried by distillation from sodium. The crystal was then dried by blowing dry compressed air over it.

Figure 6 shows several photographs of etched crystal surfaces. Plates a and b are melt-grown, plates c and d are solution-grown by convection, and plates e and f are solution-grown by evaporation. The dislocation density was determined by counting the etch pits in a .05 x .05 cm area. Etching was always done on a freshly cleaved sample and both surfaces were etched. Both surfaces were then examined; and if they matched, it was concluded that no dislocations were introduced in the cleaving or etching process. Plates a and b of Figure 7 show two matched surfaces. Since cleaving the crystal introduced dislocations at the edge of the crystal, the regions that were examined were in the center of the cleaved face. The faces of the melt-grown crystals were at least 1 x 1 cm, while the solution-grown crystals were approximately .5 x .5 cm.

As can be seen from Figure 6, the dislocation density of the solution-grown crystals is less than the melt-grown crystals. The

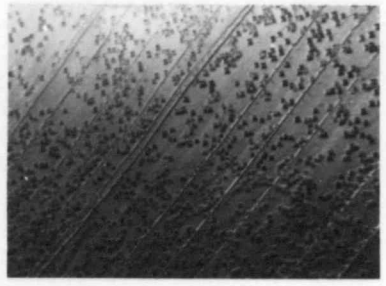

Plate a

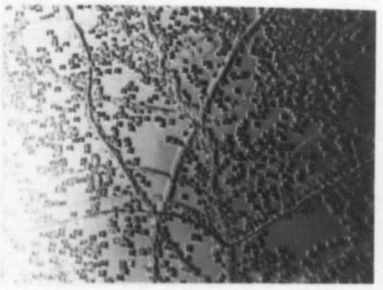

Plate b

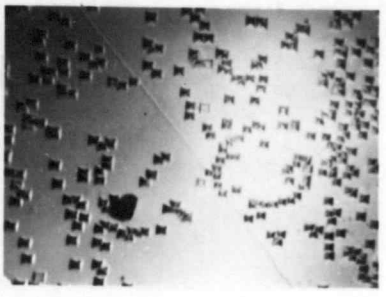

Plate c

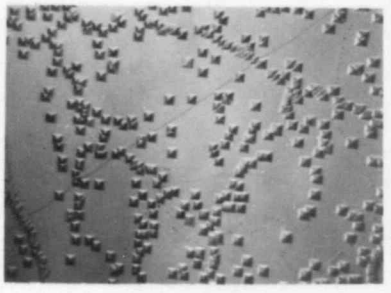

Plate d

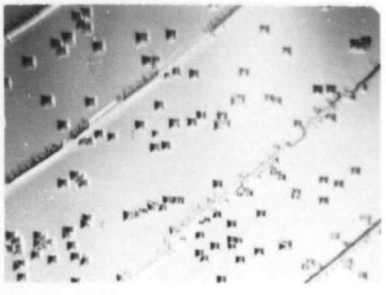

Plate e

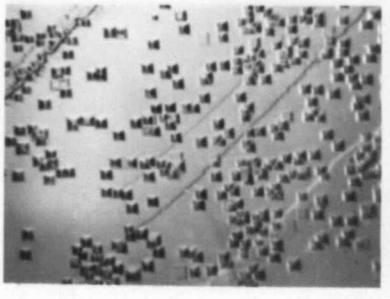

Plate f

Figure 6. Etched KCl crystals. Plates a and b are of melt-grown crystals, plates c and d are of crystals solution-grown by convection, and plates e and f are of crystals solution-grown by evaporation. (⟼ = 100 μ)

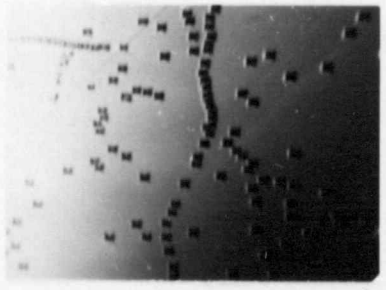

Plate a

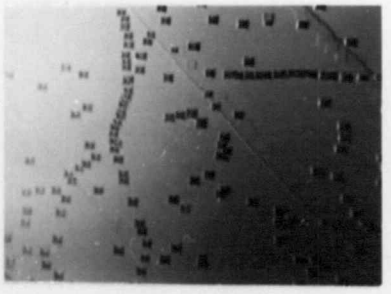

Plate b

Plate c

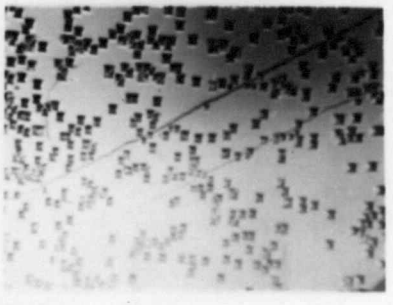

Plate d

Figure 7. Etched KCl crystals after annealing. Plates a and b are of matched melt-grown crystals, plate c is of a solution-grown crystal, and plate d is of a Harshaw crystal. (⟼ = 100 μ)

solution-grown crystals, both convection and evaporation grown, contained 8×10^4 dislocations per cm^2, while the melt grown crystals had a dislocation density of 3×10^5. The dislocation densities reported are averages for several crystals, and were found to vary by a factor of two between crystals of the same type.

Gruzensky (18) reported that sodium chloride crystals grown by evaporation contained no dislocations. Botsaris, Mason, and Reid (4) reported that pure potassium chloride crystals grown from a supersaturated solution at constant temperature contained the same number of dislocations as the seed crystal. Botsaris et al. only grew a thin layer (. 1 to . 3 mm) of potassium chloride on the seed crystal. The strain at the interface of the seed and the new material probably extended throughout the thin solution-grown region, leading to a large dislocation density.

Figure 7 also shows the effect of thermal annealing on the dislocation density of the crystals. The crystals were placed in a Vycor tube which contained an atmosphere of chlorine. The crystals to be etched were supported on potassium chloride crystals, which removed any source of strain which would be caused by the difference in thermal expansion between the samples and the support. The temperature was held at 600° C for one week, then lowered to room temperature over a period of one week. Plates a and b of Figure 7 show matching surfaces of a melt-grown annealed crystal, and plate c

shows a solution-grown annealed crystal. It was observed that the dislocation density of the solution-grown crystal was not significantly changed, while the number of dislocations in the melt-grown crystal was reduced to a value approximately equal to the solution-grown crystal.

Coloration

Gamma-Ray Source

The samples were colored in the cobalt-60 gamma-ray source shown in Figure 8. The crystal was placed in the same position in the high-flux chamber for each irradiation. The door was then opened and the rods were raised to a position surrounding the high-flux chamber. When the rods were in the raised position, the gamma-ray flux was 3×10^5 roentgens per hour.

Because the time necessary to open the door and raise the rods into the operating position was one minute, a problem arose in determining the length of an irradiation. Placing the source in operation, which required one minute, was assigned an effective irradiation length of 30 seconds. Since the same procedure was required at the termination of the irradiation, the length of the irradiation was taken as the time the rods were completely raised plus one minute.

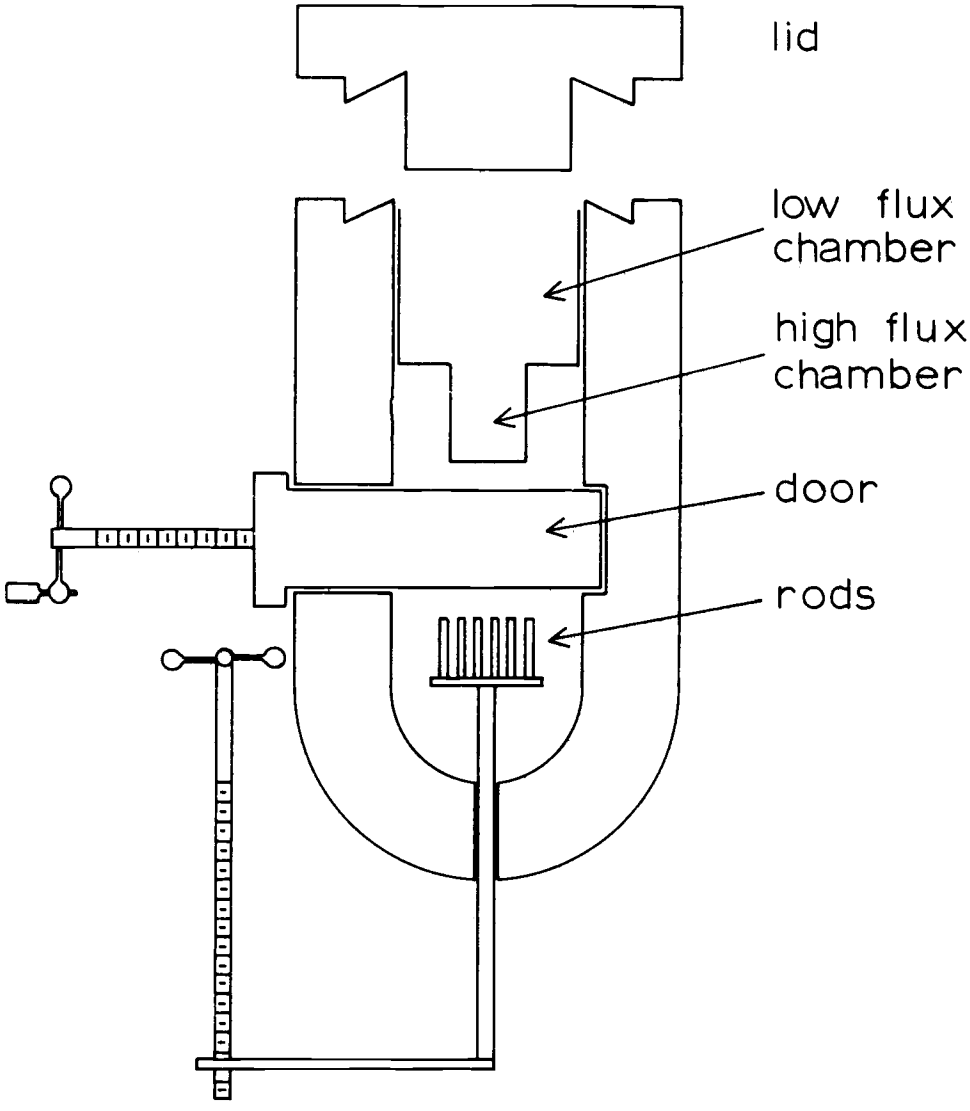

Figure 8. Cobalt-60 source.

Coloration Cell

The cell in which the crystals were irradiated has been described by Zahrt (61, p. 11-14). It was equipped with shutters so that the sample could be irradiated and then transferred to the spectrophotometer for absorbance measurements without exposing the sample to light. The potassium chloride crystal was mounted with Elmer's Glue-All on a brass holder in the cell. The absorbance in the F band was measured by means of a Beckman Model DU spectrophotometer at room temperature. All samples were at least of 7 x 7 x 1 mm dimensions and the absorbance was measured along a path length of one mm or longer.

The coloration rate depended on temperature. Since the temperature in the cobalt source was not constant, being as much as 7° C higher than room temperature for a one hour irradiation, and the room temperature varied by several degrees, it was necessary to thermostat the cell. The cell was modified so that water could be circulated through it. Water was circulated into the cobalt-60 source and through the cell from a constant-temperature bath located outside of the source. The water bath was maintained at 25° C, and the cell temperature was 25$\pm$. 5° C.

The coloration was also found to depend on the number of interruptions made in the irradiation for absorbance measurements,

probably due to thermal bleaching of the F centers when the crystal was removed from the cobalt-60 source. Therefore, in order to obtain maximum reproducibility, the same sequence of irradiation periods was employed for each crystal. The total irradiation time was ten hours. During the first hour, measurements were taken every ten minutes, followed by half-hour irradiations for the next four hours. The final five hours of the irradiation consisted of one-hour irradiations. The sample was removed from the source for 15 minutes for the absorbance measurement, and the absorbance of the F center was measured ten minutes after removal from the irradiator.

INCORPORATION OF RARE-EARTH IONS IN POTASSIUM CHLORIDE

Introduction

The radiation induced coloration of potassium chloride crystals containing rare-earth ions has not been investigated. In order to study the effect of rare-earth ions on the coloration, crystals were grown containing either europium, dysprosium, or praseodymium.

Of these rare-earth ions, only the substitution of europium into the potassium chloride lattice has been extensively studied. The absorption and luminescence has been investigated by Wagner and Bron (59) at 10° K and by Reisfeld and Glasner (42) at room temperature. The electron-spin resonance was investigated by Röhrig (46). The spectral and the electron-spin resonance results of these and other authors show that europium is present in the divalent oxidation state. A cation vacancy is present to provide charge neutrality.

Some work has been reported on the incorporation of dysprosium in potassium chloride. Hills and Scott (20) were unable to detect any dysprosium in potassium chloride crystals grown from a melt containing dysprosium chloride. Pissarenko and Voropaera (37) reported that dysprosium was present in potassium chloride when the crystals were grown from a melt of KCl and $DyCl_3$ in an atmosphere of fluorine or sulfur. From the luminescence of their material, they

concluded that the dysprosium was present in the trivalent state.

Asundi and Naik (3) and Dologopolora et al. (12) have reported the incorporation of praseodymium in the alkali halides. From the absorption and the fluorescence of their crystals, they reported that praseodymium was present in the trivalent state.

Experimental

Crystal Growth

The crystal-growing apparatus and the potassium chloride employed to grow these crystals were described previously. Europium oxide was obtained from the Michigan Chemical Corporation and was 99.9 percent pure. Praseodymium chloride and dysprosium chloride were purchased from the Fairmount Chemical Company and the Lindsay Chemical Company, respectively.

The europium oxide was converted to the chloride by heating it at 300° C in a stream of anhydrous hydrogen chloride. No pretreatment was done on the praseodymium chloride or the dysprosium chloride.

Potassium chloride and the rare-earth chloride were placed in the crystal-growing apparatus in a quartz crucible. The mixture was heated to 250° C for at least 12 hours in a vacuum to remove most of the water from the salt. The crystal-growing apparatus was

then filled with anhydrous hydrogen chloride at one atmosphere pressure, and the potassium chloride was melted. The melt was kept in contact with the hydrogen chloride for one hour to convert any oxychloride to the chloride.

At this time, the melt was clear with no suspended particles, which indicated that no insoluble oxychlorides were present. The hydrogen chloride was then replaced by argon, and the crystal was grown.

Neutron-Activation Analysis

Apparatus. The concentration of dysprosium and europium in the potassium chloride crystals was determined by neutron-activation analysis. The samples, which were contained in polyethylene vials, were irradiated in the rotating-rack of a TRIGA MARK II reactor. Irradiations were carried out for ten minutes at 100 kilowatts or for 30 minutes at 250 kilowatts, depending on the size of the sample. The reactor produced a neutron flux of 7×10^{11} neutrons sec^{-1} cm^{-2} when operated at 250 kilowatts.

The gamma-ray spectra of the samples were determined with a Technical Measurements Corporation 400 channel analyzer equipped with a 3- by 3 inch NaI(Tl) well crystal.

Chemical separation. A chemical separation of the dysprosium and the europium from the host potassium chloride was done to

remove the large activity caused by the formation of ^{42}K and ^{38}Cl isotopes. Immediately after the irradiation, the sample had a large activity because of the ^{38}Cl isotope. Since the ^{38}Cl isotope has a half-life of 37 minutes, a two hour waiting period was sufficient to reduce the activity to a level where the sample could be handled safely.

After the waiting period, the samples were dissolved in five ml of a carrier solution containing one milligram each of dysprosium and europium. Aqueous ammonia (28 percent) was added to precipitate the rare-earth hydroxide. A centrifuge was employed to separate the precipitate from the solution. The hydroxide precipitate was washed twice with a dilute ammonia solution, and then re-dissolved with 1M hydrochloric acid. The precipitation and washing was carried out a second time.

After the second precipitation, the precipitate was dissolved in hydrochloric acid and transferred to a polyethylene vial. The vial was heat-sealed and the sample was then counted.

Treatment of data. The number of micrograms of dysprosium or europium in a sample can be found directly from a comparison of the photopeak area in the sample and a standard. If A is the photopeak area of a particular element in the sample, and A_s is the corresponding photopeak area in the standard

$$C = C_s \frac{A}{A_s} e^{\frac{.693t}{t_{1/2}}}$$

where C_s and C are the number of micrograms of the element in the standard and the sample respectively, $t_{1/2}$ is the half-life of the element, and t is the time elapsed between counting the standard and the sample. A negative time is used if the sample is counted before the standard.

The photopeak area was found by assuming a linear baseline. The trapezoidal area (A_b) under the baseline was subtracted from the total photopeak area (A_t) to give the photopeak area (A). The total area (A_T) under the photopeak can be found directly from the gamma-ray spectrum by adding the counts in each channel which contribute to the photopeak. Thus

$$A_t = \sum_{n=i}^{f} N_n$$

where i and f are the initial and the final channel in the photopeak. The initial and the final channel are chosen at the minimum on each side of the photopeak, if the minimum exists, or in a region where the background slope becomes constant. The baseline area is given by

$$A_b = \frac{f-i+1}{2} (N_i + N_f)$$

where N_i and N_f are the counts in the initial and the final channel, respectively. The standard deviation of the photopeak area (A) is then given by (29, p. 72-77)

$$\sigma = \sqrt{A_t + A_b}$$

When the photopeak area is given in the data, this standard deviation will be reported.

Spectral measurements. The spectra of the crystals were recorded at room temperature on a Perkin-Elmer Model 450 spectrophotometer. The spectral region investigated was from 185 mμ to 700 mμ. None of the crystals doped with rare-earth ions exhibited any absorption at 204 mμ, indicating that there was no hydroxide present.

Results

Europium Analysis

Concentration. Five crystals were grown, each containing a different concentration of europium in the melt. Several samples were taken from each crystal, each sample being cleaved from the crystal perpendicular to the direction of growth. Figure 9 shows the position of the samples for three of the crystals. The two crystals not pictured were small, and only one sample was taken from each. The samples used for the coloration experiments were also analyzed at this time.

The europium concentration was found from the area of the .122 Mev photopeak of the 9.3 hour ^{152m}Eu isotope. The samples were counted initially about 20 hours after the irradiation, and then a

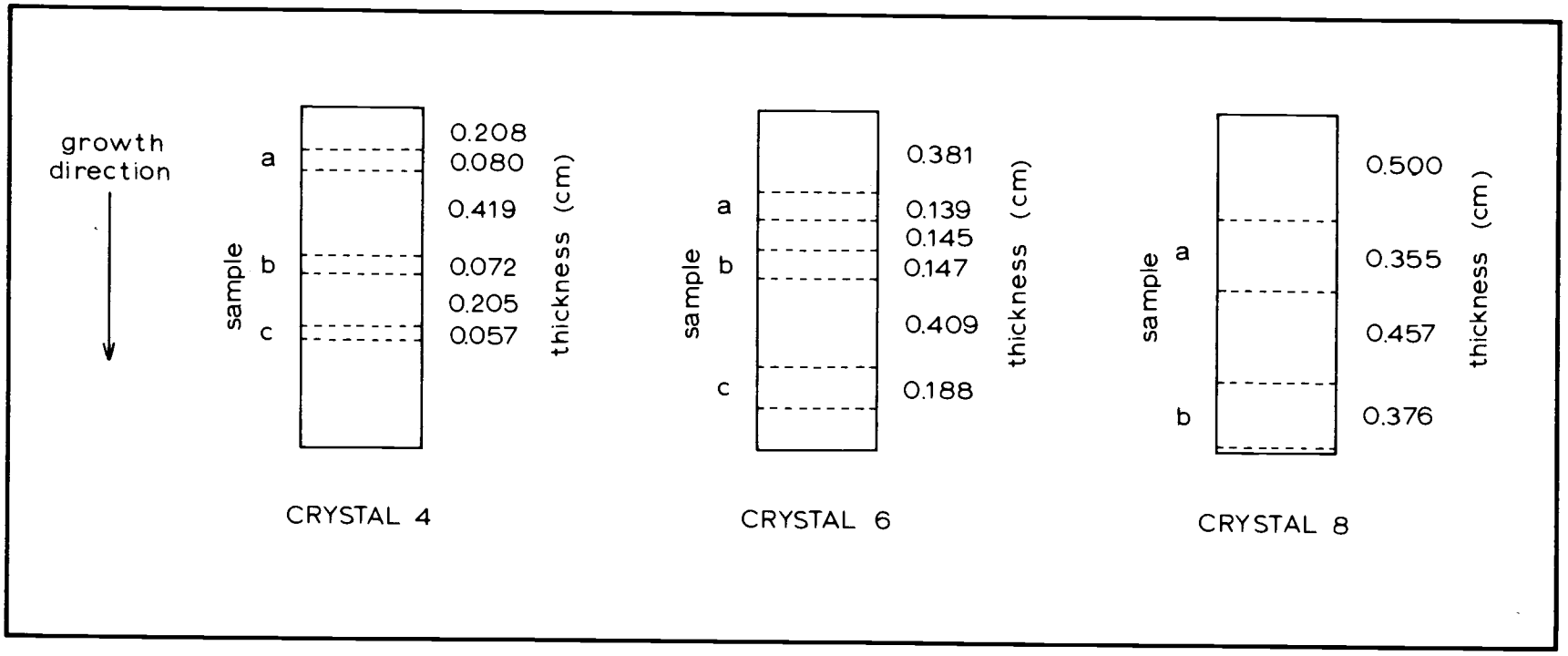

Figure 9. Position of samples taken from europium-doped crystals.

second time one day later. The samples were counted for ten minutes with the 400 channel analyzer set at five Kev per channel. The counting geometry was different in each counting series; the first time the samples were on a shelf 1/2 inch above the crystal detector, the second time they were placed in the well of the detector.

Table 1 gives the data obtained and the number of micrograms of europium in each sample. The number of micrograms is taken as the average of the two values. Table 2 gives the mole fraction of europium in each sample.

Distribution coefficient. The concentration of europium in the crystal is related to the concentration of europium in the melt by

$$D = \frac{X_c}{X_m}$$

where D is the distribution coefficient, and X_c and X_m are the mole fraction of europium in the crystal and in the melt, respectively.

The distribution coefficient was calculated for each crystal from the sample taken nearest to the top of the crystal. Table 3 shows the results of this calculation. The distribution coefficients calculated for crystals 4 and 5 are much lower than those found for the other three crystals. Since these crystals were grown from melts containing the largest concentration of europium, the maximum solubility of europium in solid potassium chloride is probably being approached. In the case of crystals 4 and 5, the growth rate was too

Table 1. Europium content of the potassium chloride samples.

Sample	Irradiation*	Series	t(hr)	A (cpm)	μg Eu	Average ± Average Deviation, μg
Eu std.	1	1		1,490 ± 20	3.00	
		2		1,810 ± 20		
Eu std.	2	1		12,940 ± 60	3.00	
		2		14,700 ± 60		
		3		3,790 ± 90		
4 a	2	1	6.93	45,160 ± 110	17.5	18.4 ± .9
		3	-1.63	27,570 ± 80	19.3	
4 b	2	1	18.7	35,030 ± 90	32.8	34.1 ± 1.3
		3	-0.72	47,080 ± 140	35.4	
4 c	2	1	18.5	38,440 ± 90	35.4	35.6 ± .2
		3	-0.45	46,230 ± 110	35.8	
5 a	2	1	2.90	53,530 ± 110	15.4	15.0 ± .4
		3	-0.95	19,760 ± 70	14.6	
5 b	2	1	2.67	36,370 ± 92	10.3	10.2 ± .1
		2	2.72	40,700 ± 100	10.2	
6 a	2	1	2.45	16,560 ± 60	4.61	4.65 ± .04
		2	1.80	20,420 ± 70	4.68	
6 b	1	1	2.45	3,820 ± 30	9.27	9.23 ± .04
		2	2.70	4,550 ± 30	9.19	
6 c	1	1	2.22	7,490 ± 40	17.8	17.7 ± .1
		2	3.18	8,420 ± 40	17.6	
6 d	2	1	1.58	23,370 ± 70	6.10	6.38 ± .28
		2	2.03	28,040 ± 90	6.66	
7 a	1	1	1.60	600 ± 13	1.36	1.39 ± .03
		2	1.60	760 ± 15	1.42	
7 b	1	1	1.42	890 ± 15	2.01	1.97 ± .04
		2	1.02	519 ± 15	1.93	
7 c	2	1	1.02	2,150 ± 20	0.537	0.545 ± .009
		2	0.22	1,190 ± 20	0.554	
8 a	1	1	1.02	440 ± 17	0.97	1.00 ± .04
		2	1.22	570 ± 17	1.04	
8 b	1	1	0.62	470 ± 12	1.01	1.03 ± .02
		2	1.80	550 ± 18	1.05	
8 c	2	1	0.22	960 ± 22	0.226	0.240 ± .014
		2	0.42	1,200 ± 30	0.254	

* 1 corresponds to an irradiation for ten minutes at 100 Kilowatts,
2 corresponds to an irradiation for 30 minutes at 250 Kilowatts.

Table 2. Mole fraction, X_c, of europium in the potassium chloride samples.

Sample	Sample Mass (g)	μg Eu	$X_c \pm$ Average Deviation
4 a	0.0775	18.4 ± .9	$1.16 \pm .06 \times 10^{-4}$
4 b	0.1200	34.1 ± 1.3	$1.39 \pm .05 \times 10^{-4}$
4 c	0.1010	35.6 ± .2	$1.73 \pm .01 \times 10^{-4}$
4 d	0.0655	12.3 ± 1.9	$9.2 \pm 1.4 \times 10^{-5}$
5 a	0.1097	15.0 ± .4	$6.71 \pm .18 \times 10^{-5}$
5 b	0.0668	10.2 ± .1	$7.49 \pm .07 \times 10^{-5}$
6 a	0.1207	4.65 ± .04	$1.89 \pm .02 \times 10^{-5}$
6 b	0.2060	9.23 ± .04	$2.20 \pm .01 \times 10^{-5}$
6 c	0.3617	17.7 ± .1	$2.40 \pm .02 \times 10^{-5}$
6 d	0.1516	6.38 ± .28	$2.06 \pm .09 \times 10^{-5}$
7 a	0.3130	1.39 ± .03	$2.18 \pm .05 \times 10^{-6}$
7 b	0.4266	1.97 ± .04	$2.27 \pm .05 \times 10^{-6}$
7 c	0.1262	0.545 ± .009	$2.12 \pm .04 \times 10^{-6}$
8 a	0.8041	1.00 ± .04	$6.10 \pm .24 \times 10^{-7}$
8 b	0.7081	1.03 ± .02	$7.14 \pm .14 \times 10^{-7}$
8 c	0.1555	0.240 ± .014	$7.57 \pm .45 \times 10^{-7}$

fast to incorporate the large equilibrium amount of europium in the crystal. This resulted in a distribution coefficient which was too small.

Table 3. Distribution coefficient, D, for europium.

Crystal	Sample	$X_m \times 10^4$	$X_c \times 10^4$	D
4	a	35.4	1.16	0.0328
5	a	6.65	0.671	0.101
6	a	0.879	0.189	0.215
7	a	0.096	0.0218	0.23
8	a	0.033	0.00610	0.18
Average and standard deviation				0.21±.03*

*Includes only last three results

Spectra. The spectra of two crystals containing europium are shown in Figure 10. At room temperature the spectrum consists of two broad bands, each containing several unresolved peaks. This is in agreement with the results of Reisfeld and Glasner (42).

The low energy band consists of three peaks, the strongest being at 325 mμ. The high energy band consists of at least four peaks. At a low concentration of europium the high energy band does not show any fine structure.

Molar absorptivity. The absorbance of europium in the potassium chloride crystals can be related to the concentration of europium

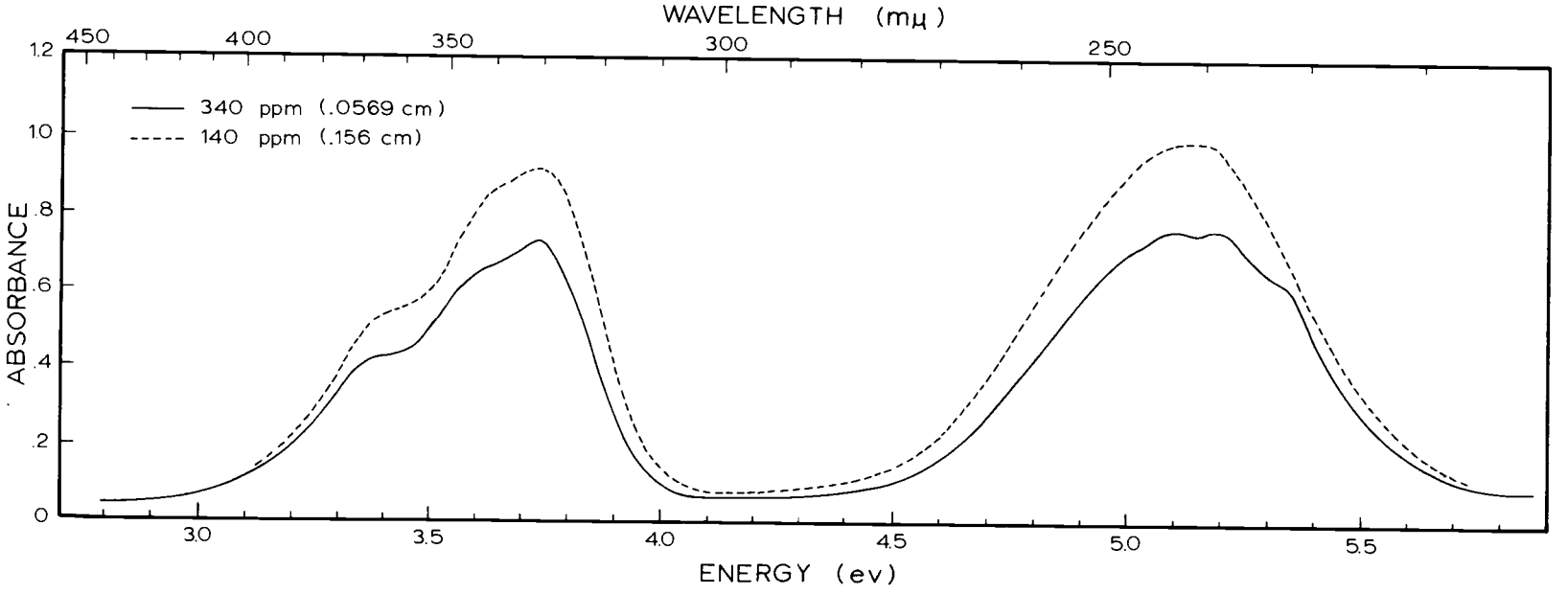

Figure 10. Absorption spectra of europium in KCl at room temperature.

at a particular wavelength by the Beer-Lambert law. Expressed mathematically the law is

$$A_\lambda = \varepsilon_\lambda bc$$

where A_λ is the absorbance ($\log_{10} \frac{I_o}{I}$) at the wavelength λ, ε_λ is the molar absorptivity, c is the concentration of europium in moles per liter, and b is the sample thickness.

Figure 11 gives a plot of the absorbance per centimer at 241 mμ against the mole fraction of europium. The graph is linear over the range studied, therefore, the Beer-Lambert law is valid.

Table 4 gives the results for the calculation of the molar absorptivity at two wavelengths. The wavelengths chosen were 241 mμ and 325 mμ, which are the maxima of the high- and of the low-energy bands respectively. Crystals seven and eight were not averaged with the other results because of the large error in the absorbance at very low europium concentrations.

If the concentration has units of mole fraction, ε_{241} and ε_{325} are $7.39 \pm .51 \times 10^4$ and $7.05 \pm .45 \times 10^4$ cm^{-1}, respectively.

Dysprosium Analysis

Concentration. The concentration of dysprosium in the potassium chloride samples was determined by integrating the area under the .098 Mev photopeak of ^{165}Dy. The 400-channel analyzer was

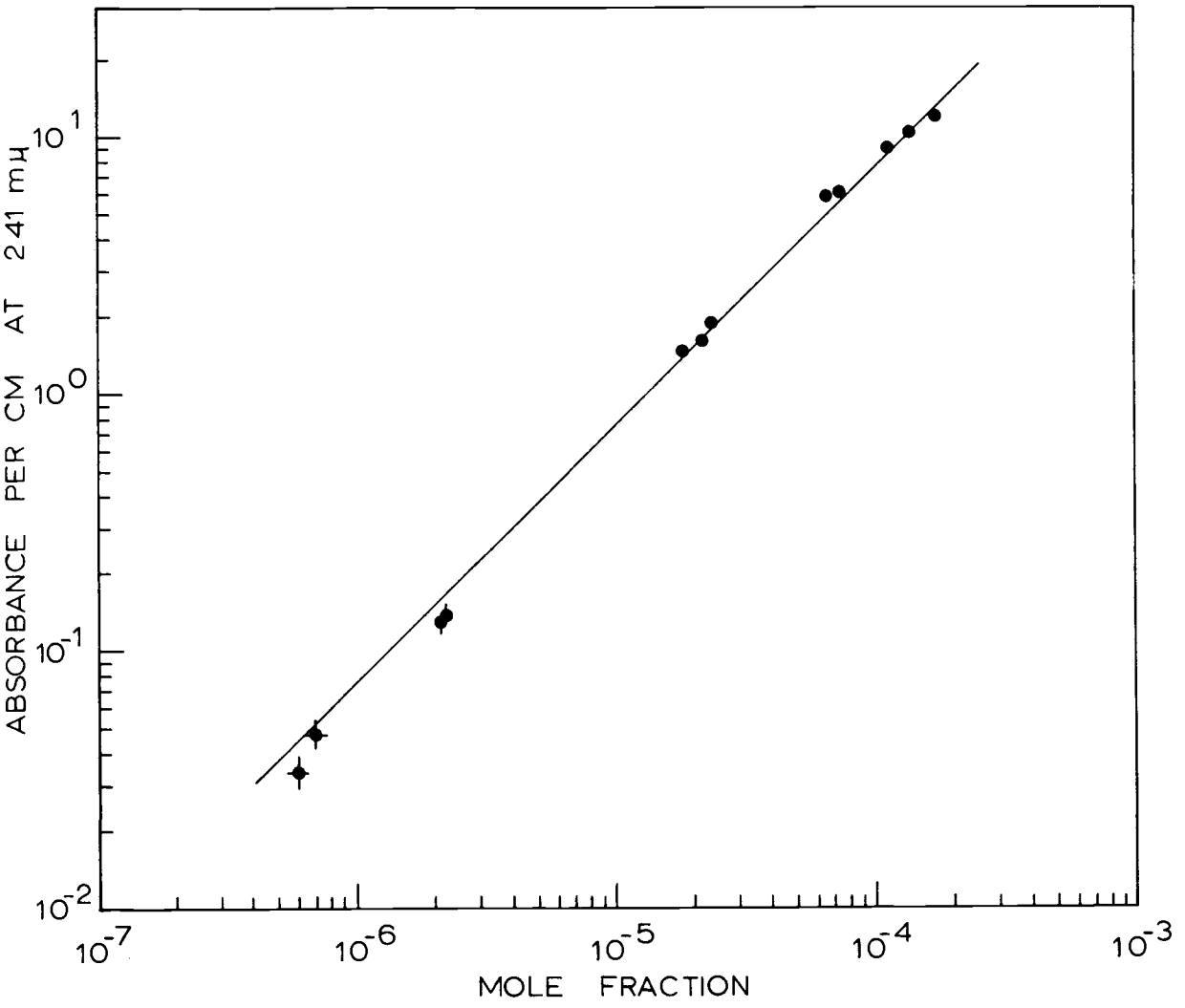

Figure 11. Relation between absorbance and concentration of europium in KCl.

Table 4. Molar absorptivity of europium in potassium chloride.

Sample	C (moles per liter)	Thickness (cm)	A_{241}	A_{235}	$\varepsilon_{241} \times 10^{-3}$ (liter mole^{-1} cm^{-1})	$\varepsilon_{325} \times 10^{-3}$ (liter mole^{-1} cm^{-1})
4 a	3.09×10^{-3}	0.0801	.703	.682	2.85	2.76
4 b	3.70×10^{-3}	0.0722	.738	.717	2.76	2.69
4 c	4.60×10^{-3}	0.0569	.681	.672	2.60	2.56
5 a	1.78×10^{-3}	0.1559	.906	.860	3.26	3.09
5 b	1.99×10^{-3}	0.0767	.465	.433	3.04	2.83
6 a	5.03×10^{-4}	0.1389	.202	.190	2.89	2.72
6 b	5.85×10^{-4}	0.1467	.235	.220	2.74	2.56
6 c	6.38×10^{-4}	0.1884	.351	.333	2.93	2.77
7 a	5.80×10^{-5}	0.4619	.060	.062	2.2	2.3
7 b	6.04×10^{-5}	0.2883	.040	.041	2.3	2.4
8 a	1.62×10^{-5}	0.3551	.012	.013	2.1	2.3
8 b	1.90×10^{-5}	0.3755	.018	.018	2.5	2.5
*Average and standard deviations					$2.88 \pm .20$	$2.75 \pm .17$

*Does not include last four results.

operated at ten Kev per channel. The photopeak maximum was in Channel 11, and the integration was from channel 8 through channel 16.

The standards contained one microgram of dysprosium and in both standards a small quantity of europium was detected. One of the ^{152m}Eu photopeaks is at .122 Mev and this would contribute to the dysprosium photopeak at .098 Mev. It is therefore necessary to correct the .098 Mev photopeak for the europium activity.

Dysprosium does not have any photopeaks in the .74 to 1.16 Mev region, while europium has several (.841, .963 and .975 Mev). The ratio of the area in the .098 Mev region to the area in the .74 to 1.16 Mev region was determined from the europium standards. Then by determining the area in the .74 to 1.16 Mev region for the dysprosium standards, the activity of the europium in the .098 Mev region was found. This activity was subtracted from the total .098 Mev photopeak to give the true dysprosium activity. Table 5 gives the result of this calculation.

Table 5. Correction of the dysprosium standards.

Sample	Irradiation Conditions	A_t (cpm)	A_b (cpm)	Eu Correction (cpm)	A (cpm)
1	100 Kev., 10 min.	42,719.6	14,515.7	6,653.7	21,550 $\pm$ 80
2	250 Kev., 30 min.	37,508.6	12,483.9	4,399.7	20,625 $\pm$ 73

The separation of the dysprosium from the potassium chloride matrix was not complete; there was always a small 1.64 Mev photopeak due to ^{42}K observable in the gamma-ray spectra. The ^{42}K isotopes will contribute to the area of the .098 Mev photopeak since the gamma-ray spectrum of ^{42}K is not linear in this region. Figure 12 shows the gamma-ray spectra of two dysprosium samples, each counted several hours apart. In the second spectrum of each, there is still a considerable area in the .098 Mev region. Since ^{165}Dy has a half-life of 2.3 hours, the area of the photopeak should be less than the area that is observed.

If we assume that the total area in the .098 Mev photopeak is due only to the ^{42}K and ^{165}Dy isotopes, we can correct for the activity of ^{42}K. Each sample was counted twice. Let A_i and A_f be the area of the .098 Mev photopeak when counted the first and the second time, respectively. Then.

$$A_i = A_i^{Dy} + A_i^{K}$$

where A_i^{Dy} and A_i^{K} are the areas due to dysprosium and potassium, respectively. And

$$A_f = A_i^{Dy} e^{-\lambda_{Dy} t} + A_i^{K} e^{-\lambda_{K} t}$$

where t is the time elapsed between counting the samples, and λ is .693 divided by the half-life of the ^{165}Dy or ^{42}K isotopes. Then solving the above for the initial area of the .098 Mev photopeak due to

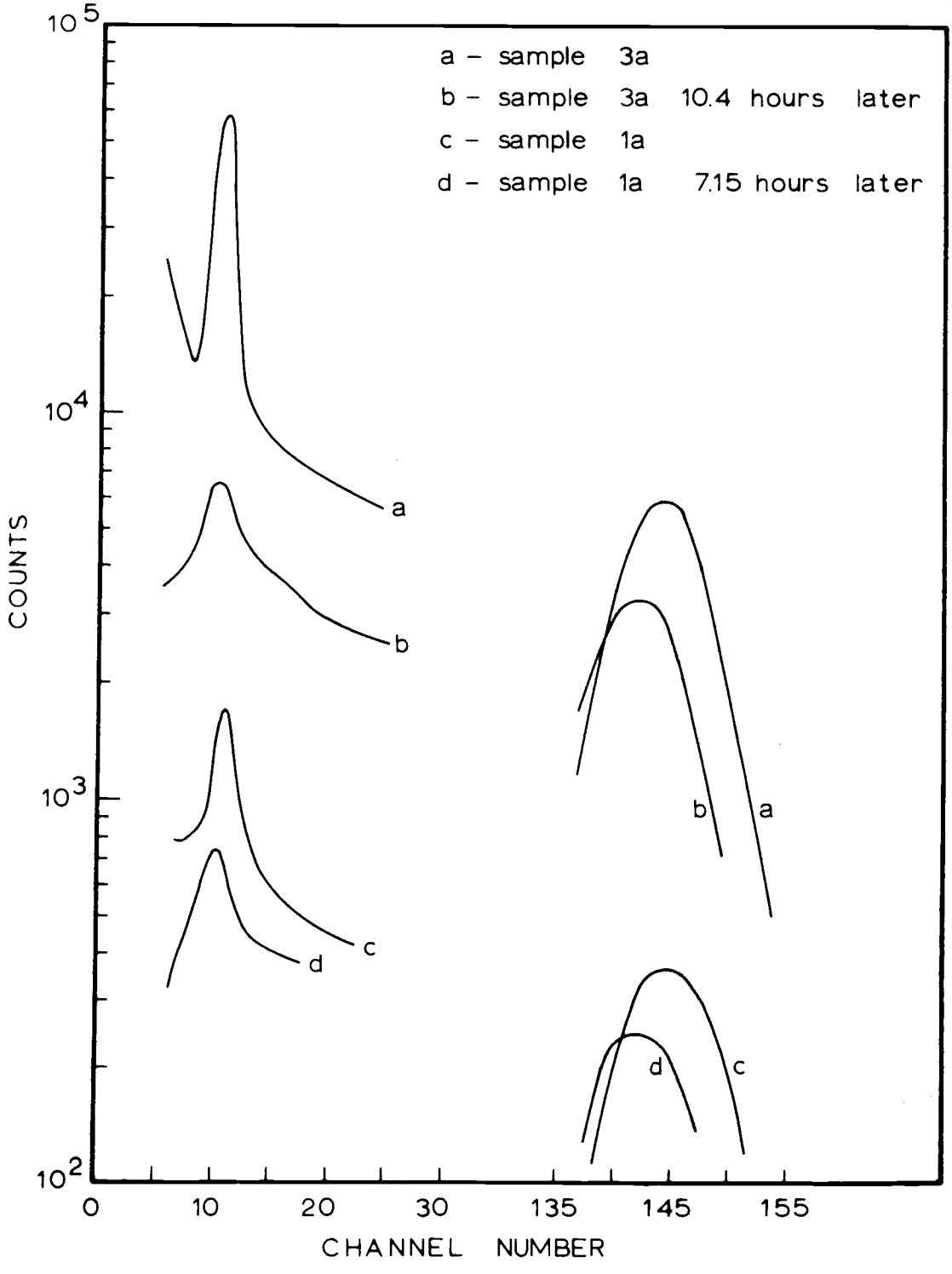

Figure 12. Gamma-ray spectra of two dysprosium samples. The counting interval was ten minutes.

dysprosium we find

$$A_i^{Dy} = \frac{A_i \, e^{-\lambda_K t} - A_f}{e^{-\lambda_K t} - e^{-\lambda_{Dy} t}}$$

Table 6 gives the results of the above correction. The errors reported are due to counting statistics only.

Table 7 gives the mole fraction of dysprosium in the samples. Figure 13 shows the position of several of the samples. The concentration of dysprosium in the samples increased as the sample was removed from a position lower in the crystal. This is expected, because as the crystal grows, the melt becomes more concentrated in dysprosium. Notice that sample 3 c was removed directly above the precipitated region. The mole fraction of this sample was 5.21×10^{-6}; this is the maximum concentration of dysprosium that can be incorporated in crystals grown by the Kyropoulous method.

Distribution coefficient. The distribution coefficient was calculated for each crystal from the sample taken nearest the top of the crystal. Table 8 shows the results.

Spectra. None of the crystals exhibited any absorption bands in the region 185 mμ to 700 mμ. The luminescence of dysprosium in potassium chloride has been reported by Pissarenko and Voropaeva (37) but the crystals grown in this laboratory gave no luminescence. Since their crystals were grown from melts under an atmosphere of

Table 6. Correction of the .098 Mev ^{165}Dy photopeak area.

Sample	t (hour)	A_i (cpm)	A_f (cpm)	A_i^{Dy} (cpm)
1 a	7.15	226 ± 12	56 ± 10	175 ± 23
1 b	8.15	1,372 ± 48	713 ± 38	290 ± 49
1 c	8.92	1,840 ± 51	741 ± 39	704 ± 84
1 d	8.10	1,743 ± 46	675 ± 37	796 ± 87
2 a	6.23	4,057 ± 56	1,356 ± 45	2,760 ± 110
2 b	7.07	5,116 ± 62	1,598 ± 49	3,370 ± 120
2 c	9.33	10,110 ± 58	1,101 ± 33	9,250 ± 90
2 d	7.68	2,598 ± 42	703 ± 31	1,806 ± 67
3 a	10.38	9,395 ± 54	792 ± 28	8,708 ± 81
3 b	5.63	6,968 ± 57	2,473 ± 40	4,842 ± 110
3 c	5.00	12,579 ± 62	3,322 ± 42	11,740 ± 120
3 d	8.33	2,999 ± 34	426 ± 22	2,690 ± 59

Table 7. Concentration of dysprosium in the potassium chloride samples.

Sample	Irradiation Condition*	Time (hour)	μg Dy	Sample Weight (gram)	$X_c \times 10^6$ (mole fraction)
1 a	1	5.58	0.0422 ± .0055	.4948	0.0391 ± .0051
1 b	1	5.80	0.074 ± .013	.5830	0.0585 ± .0099
1 c	1	6.23	0.205 ± .024	.9287	0.101 ± .012
1 d	2	-1.68	0.0237 ± .0026	.1193	0.0909 ± .0099
2 a	1	7.13	1.049 ± .042	1.0796	0.446 ± .018
2 b	1	7.08	1.261 ± .044	.9733	0.594 ± .021
2 c	1	6.02	2.530 ± .025	.6220	1.87 ± .02
2 d	1	6.87	0.635 ± .023	.5197	0.561 ± .021
3 a	1	5.17	1.85 ± .02	.5322	1.60 ± .01
3 b	1	7.70	2.18 ± .05	.5913	1.69 ± .04
3 c	1	8.12	5.97 ± .06	.5256	5.21 ± .05
3 d	1	6.45	0.835 ± .018	.3647	1.05 ± .02

* 1 corresponds to an irradiation of ten minutes at 100 Kilowatts,
2 corresponds to an irradiation of 30 minutes at 250 Kilowatts.

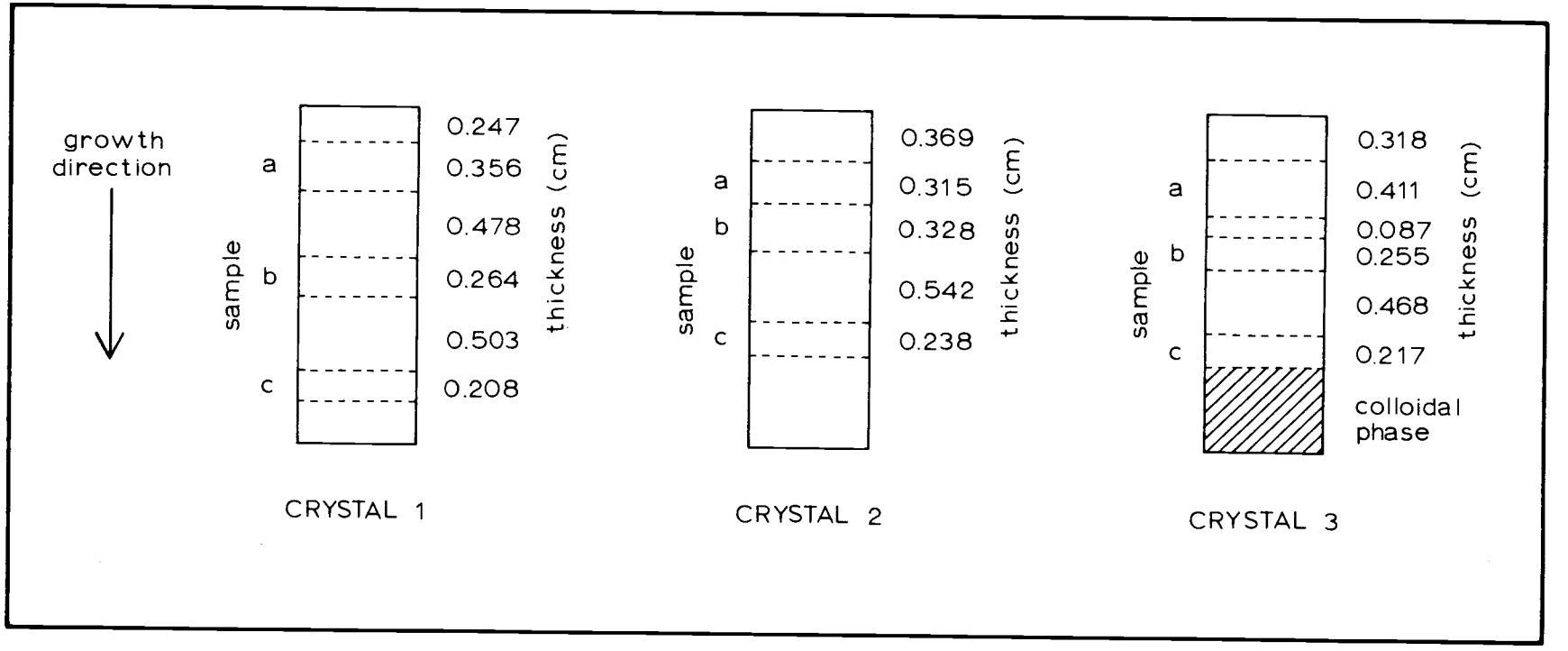

Figure 13. Position of samples taken from dysprosium-doped crystals.

Table 8. Distribution coefficient of dysprosium between molten and solid potassium chloride.

Sample	$X_m \times 10^2$	$X_c \times 10^6$	$D \times 10^5$
1 a	0.0469	0.0391	8.34
2 a	0.257	0.446	17.4
3 a	1.10	1.60	14.5
Average and standard deviation			13.4 ± 4.6

fluorine or sulfur, the dysprosium may have been incorporated in a different manner from that in pure potassium chloride.

Praseodymium in Potassium Chloride

No concentration analysis was done on the crystals doped with praseodymium because different experimental methods would have been required to count the beta particles. However, some praseodymium was incorporated into the crystals as shown by the absorbance measurements. Figure 14 shows the absorbance of one of the crystals. There is a band in the ultraviolet composed of two unresolved peaks, one at 235 mμ and the second at approximately 225 mμ.

In these crystals there is also a small band at 272 mμ. This is the wavelength at which lead absorbs in potassium chloride. In order to show that this band was due to lead ion, the luminescence was measured. The crystal was irradiated with light having a wavelength

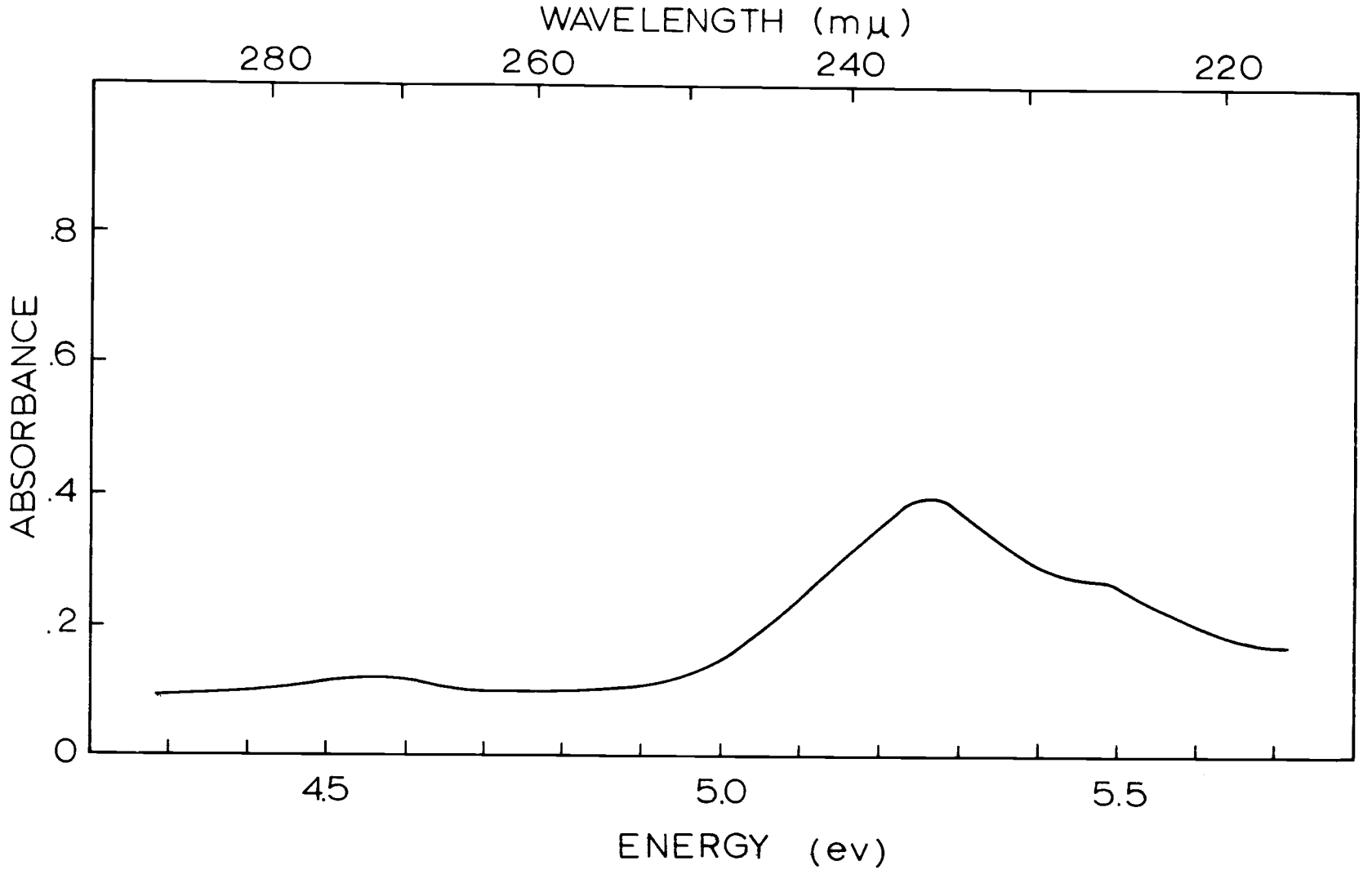

Figure 14. Spectrum of praseodymium in KCl.

of 272 mμ. The crystal exhibited a luminescence peak at 345 mμ, which is the position of the emission peak of lead. The praseodymium chloride used to dope the potassium chloride must have contained some lead.

The amount of lead in the crystals was very small. The peak height is always a factor of 30 less than the praseodymium peak. Using the value of .11 for the oscillator strength of the lead ion (21, p. 73-84; 52), the maximum concentration of lead in the potassium chloride crystals was found to be 4×10^{-8} mole fraction.

The absorption of these crystals is completely different from the spectrum of praseodymium reported by Asundi and Naik (3). However, they reported that their measurements were done while the crystal was still contained in the Vycor growing tube. It is possible that some praseodymium was incorporated in the Vycor.

RESULTS AND DISCUSSION

Coloration of Melt-Grown Doped KCl Crystals

Purpose

The effect of five cations on the gamma-ray coloration of potassium chloride was investigated. Each cation impurity was studied at several different concentrations for the purpose of determining whether some correlation exists between the impurity concentration and the gamma-ray coloration during the first and second stage.

Previously, Fröhlich and Altrichter (16) have studied the gamma-ray coloration of NaCl and KCl at several different concentrations of calcium ions. They showed that the coloration curves could be fitted to the equation derived by Mitchell, Wiegand, and Smoluchowski (31). The suppression of the gamma-ray coloration of KCl containing lead ions, at doses much larger than employed in this work, has been observed by Sibley, Sonder, and Butler (52). The coloration of alkali halide cyrstals containing rare-earth ions has not previously been investigated.

Results

Impurity concentration and coloration curves. Divalent lead

ions in potassium chloride have an absorption band at 272 mμ which is called the A band. Holmes (21, p. 73-84) and Sibley, Sonder, and Butler (52) have shown that the area of this band is proportional to the concentration of lead ions in the crystal. Employing the values of the constants for the A band reported by the above authors, Dexter's modification (10) of Smakula's equation (53) reduces to

$$N_o = 2.3 \times 10^{16} A_m$$

where N_o is the concentration of lead ions per cc and A_m is the absorbance per cm at the A band maximum. Table 9 gives the concentration of lead in each crystal sample and the coloration curves are shown in Figure 15.

The coloration experiments were done on the samples listed in Table 9 after the spectrophotometric determination of the lead content. However, the lead concentration of sample 17 was determined from the large piece of crystal listed in Table 9 and then sample 17 was removed from the center of this large piece.

Table 9. Lead-ion concentration in the KCl:Pb samples.

Sample	Absorbance at 273 mμ	Thickness (cm)	A_m (cm^{-1})	$N_o \times 10^{-16}$ (ions cc^{-1})	$X_{Pb} \times 10^6$ (mole fraction)
13	2.81	.127	22.1	51	32
14	1.53	.161	8.40	19	12
15	.189	.192	.983	2.3	1.4
16	.145	.207	.700	1.6	1.0
17	.149	1.036	.144	.33	.21
18	.0106	.254	.042	.10	.06

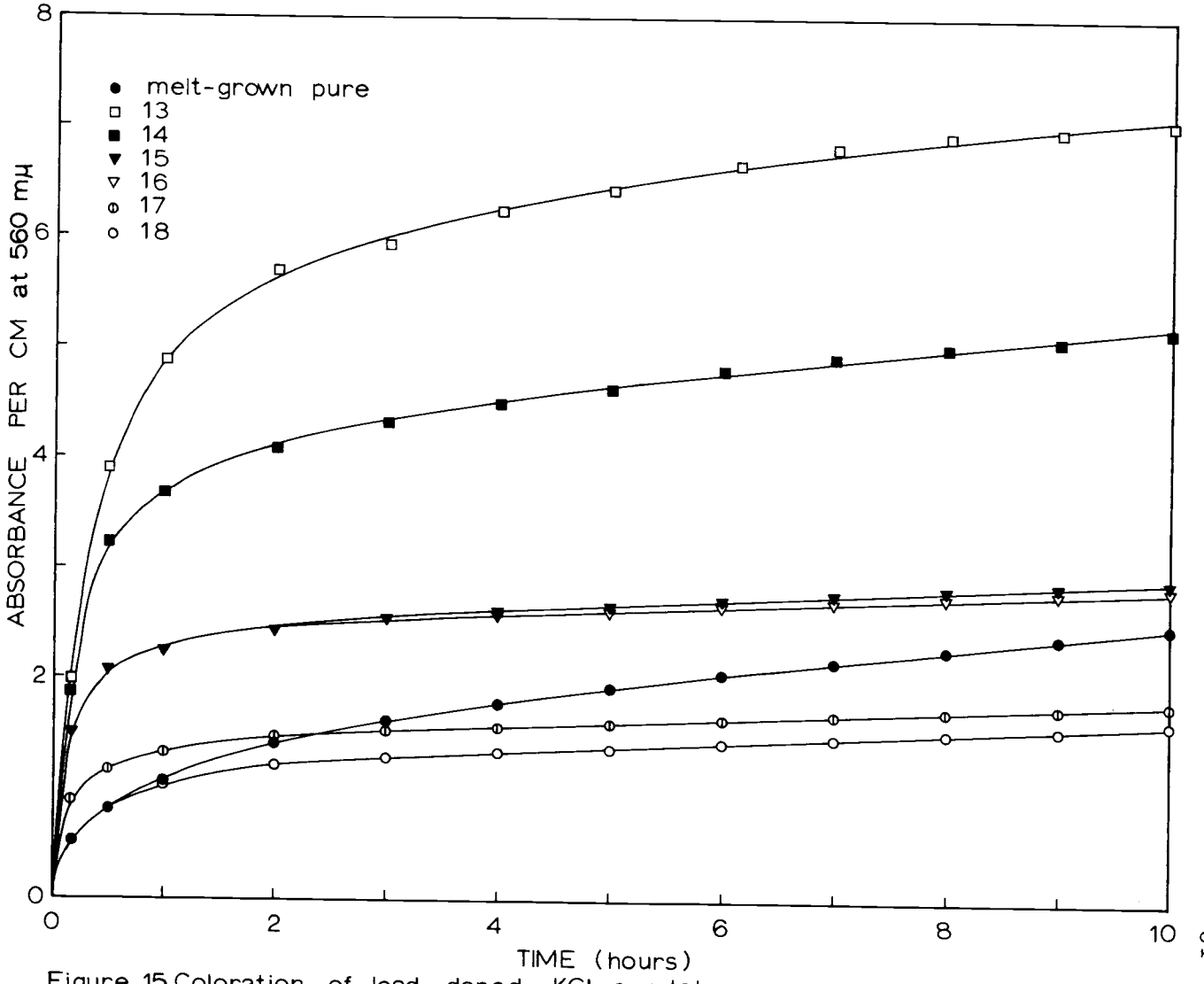

Figure 15. Coloration of lead-doped KCl crystals.

The concentration of calcium ions in the crystal samples was determined from the concentration of calcium present initially in the melt from which the crystals were grown. Kelting and Witt (25) have shown that the distribution coefficient is approximately 0.1, therefore the concentration of calcium in the crystal is about one-tenth the concentration in the melt. Table 10 gives the concentration of calcium ions in the samples used for the coloration experiments and Figure 16 shows their coloration curves.

Table 10. Concentration of calcium ions in the KCl:Ca samples.

Sample	Mole Fraction in Melt x 10^6	Mole Fraction in Crystal x 10^6	N_o x 10^{-16} (ions cc^{-1})
25	97	10	15
26	29	3	5
27	7.7	.8	1

The concentration of europium and dysprosium in the crystal samples employed for the coloration experiments was determined by neutron-activation analysis and the method has been previously described. The concentration of praseodymium in the crystals doped with praseodymium chloride was not determined; however, the relative concentration of praseodymium in the samples used for the coloration experiments could be found from the concentration of praseodymium chloride in the melt. The samples employed for the

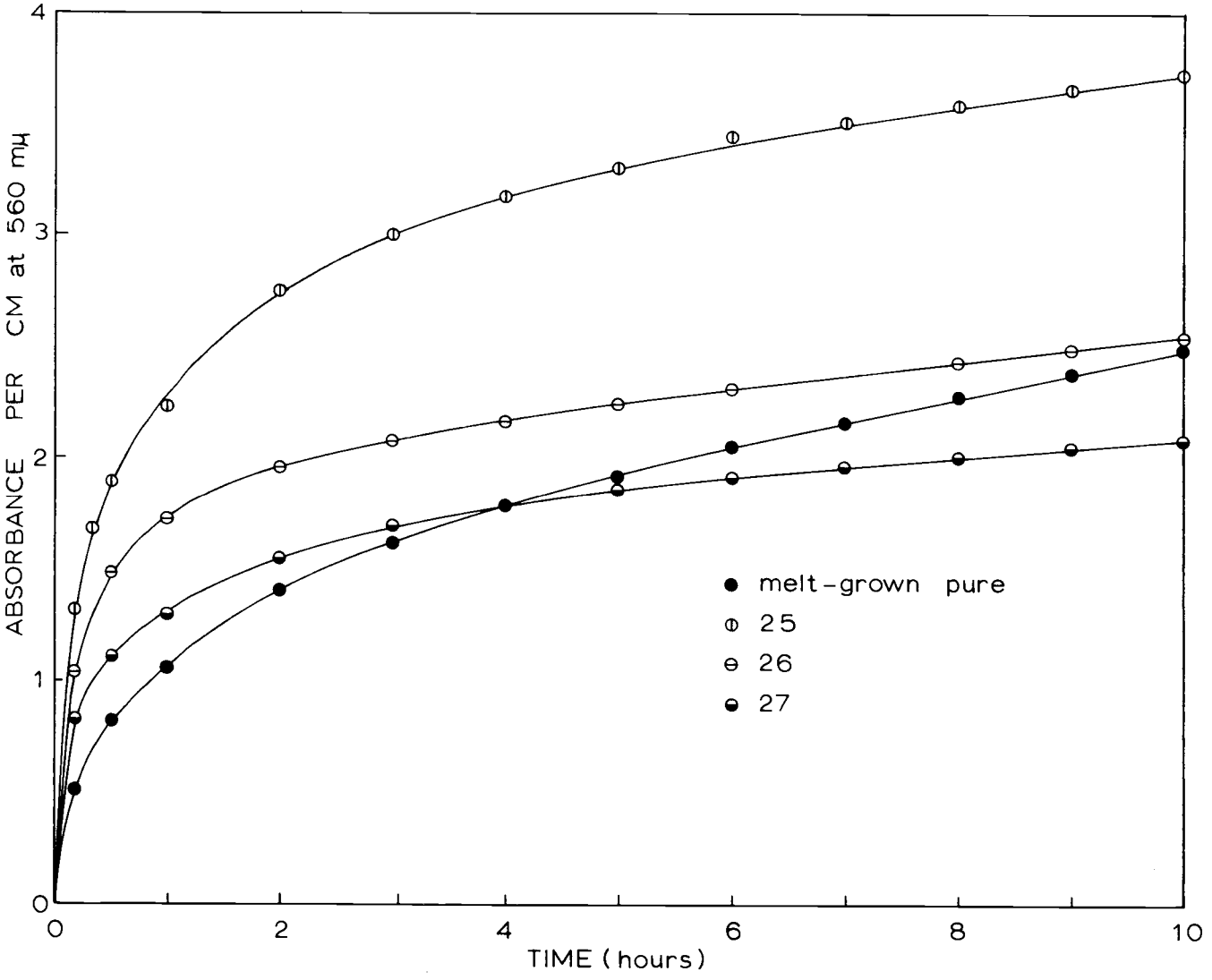

Figure 16. Coloration of calcium-doped KCl crystals.

coloration experiments were removed from the top of the praseodymium-doped crystals; therefore, if the distribution coefficient is constant over the range of concentrations employed, the concentration of praseodymium in the crystal samples will be directly proportional to the concentration of praseodymium chloride in the melt. Table 11 gives the relative praseodymium concentration in these samples.

Table 11. Relative concentration of praseodymium in the KCl:Pr samples.

Sample	Mole Fraction Pr in Melt x 10^5	Relative Pr Concentration
9	410	>170
10	92	38
11	17	7.1
12	2.4	1.0

Sample 9 was removed from the bottom of a crystal, adjacent to a region in which the praseodymium chloride had formed a colloidal precipitate. Since the impurity concentration increases as the crystal is withdrawn from the melt, sample 9 will have a relative concentration greater than the value of 170 at the top of the crystal.

Figures 17, 18, and 19 show the coloration curves for the rare-earth doped crystal samples. The concentration of europium and dysprosium have been listed previously in Tables 2 and 7, respectively.

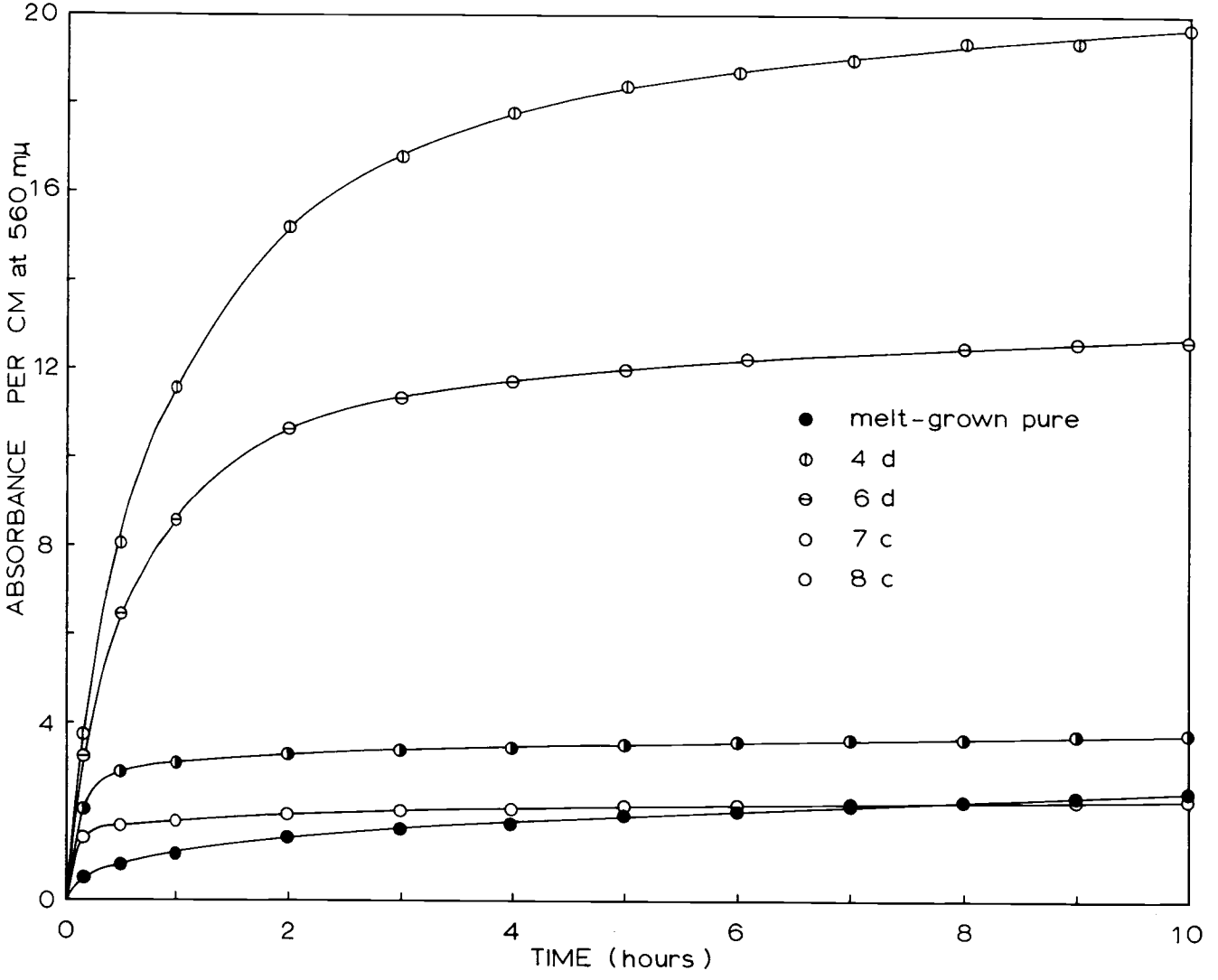

Figure 17. Coloration of europium-doped KCl crystals.

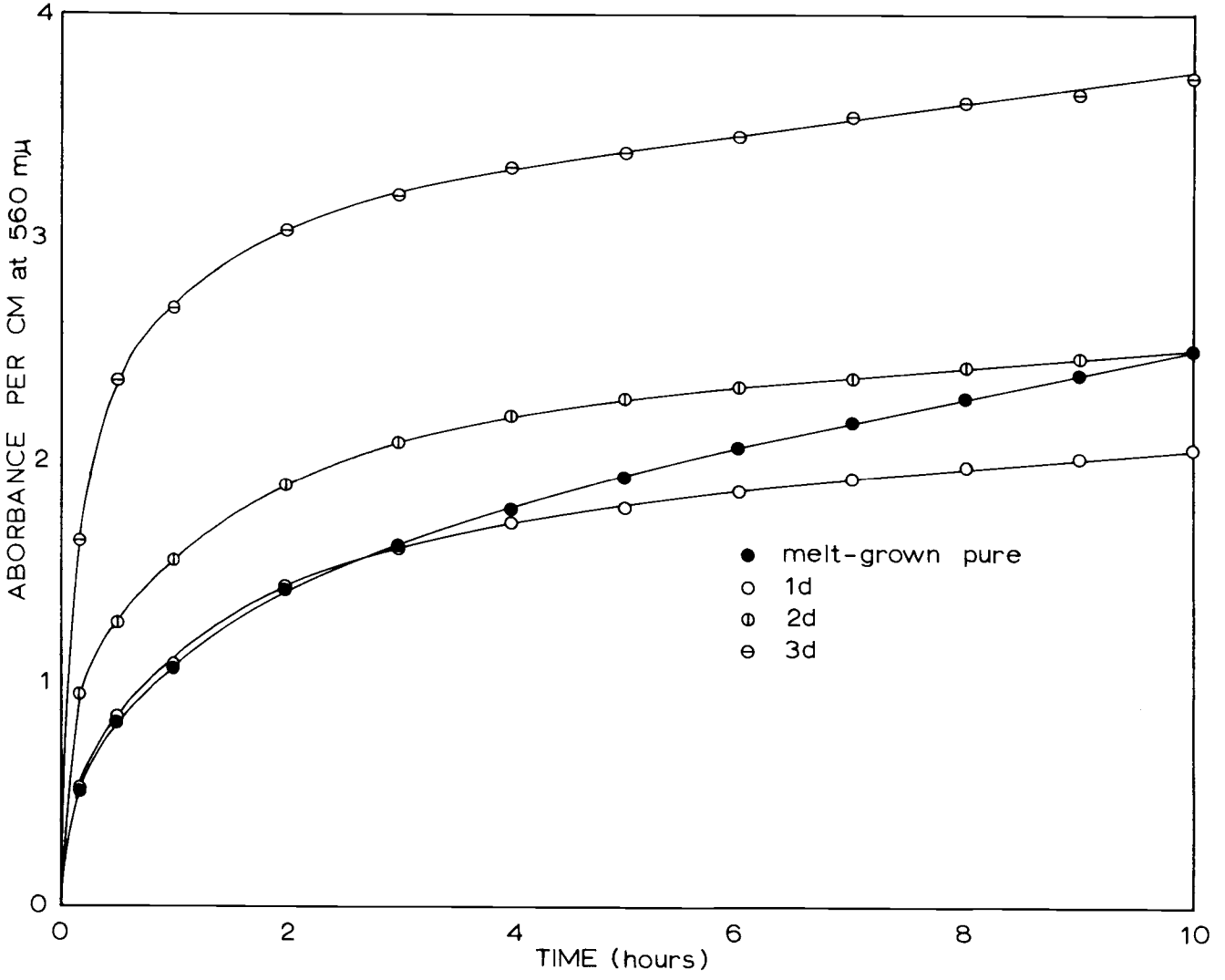

Figure 18.Coloration of dysprosium-doped KCl crystals.

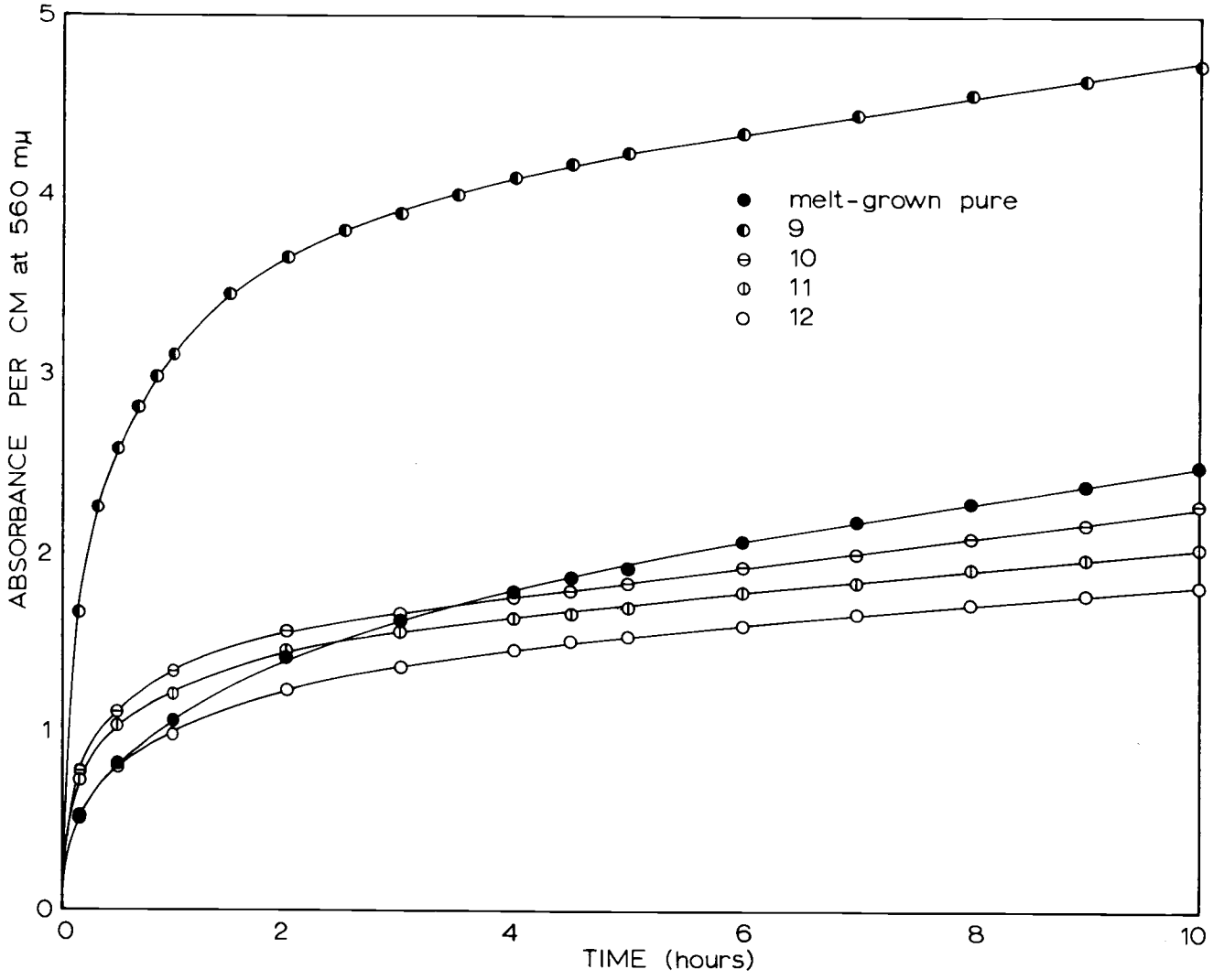

Figure 19. Coloration of praseodymium-doped KCl crystals.

Analysis of coloration curves. The coloration curves were fitted to the equation derived by Mitchell, Wiegand, and Smoluchowski using a Control Data Corporation Model 3300 computer with a standard least-squares curve-fit program. The coloration curves could be fitted to within one percent, although the values of the parameters are only accurate to approximately ten percent. Table 12 gives the values obtained for the parameters for the various crystal samples.

The total first-stage coloration is also shown in Table 12 and it was obtained directly from the coloration curves by extrapolating the linear region of the curve to the origin. This method was more accurate than using the parameters obtained from the curve-fitting procedure because of the large error in the values of the parameters.

Discussion

General effect of impurities. The five cation impurities investigated altered the growth curve of potassium chloride in the same manner, although the magnitude of the effect at a given impurity concentration depended on the impurity present. The first-stage coloration was increased by the addition of the cation impurities, however, at impurity concentrations below approximately 1×10^{16} ions per cc the increase in the coloration was very small.

The rate of second-stage coloration, given by a* in Table 12, varied with the impurity concentration in a more complex manner.

Table 12. Coloration-curve parameters for the doped crystals.

Sample	Impurity	Impurity Concentration (ions $cc^{-1} \times 10^{-16}$)	First-stage Coloration (F-centers $cc^{-1} \times 10^{-16}$)	$a^* \times 10^{-16}$ (F-centers $cc^{-1} hr^{-1}$)	$n_o^* \times 10^{-16}$ (F-centers cc^{-1})	b^* (hr^{-1})	$n_o' \times 10^{-16}$ (F-centers cc^{-1})	c^* (hr^{-1})
Melt-grown								
pure	--	--	1.38	.104	.50	8.9	1.1	.67
8 c	Eu	1.22	1.91	.026	1.52	13.3	.48	.60
7 c	Eu	3.40	3.22	.037	2.75	7.7	.60	.58
6 d	Eu	33.0	11.3	.136	2.98	5.8	8.1	1.08
4 d	Eu	147	16.9	.212	4.27	4.0	13.0	.77
1 d	Dy	.14	1.53	.045	.48	10.3	1.13	.72
2 d	Dy	.90	2.02	.036	.88	15.4	1.23	.68
3 d	Dy	1.68	2.99	.062	1.84	8.7	1.19	.96
12	Pr	1.0+	1.21	.055	.52	9.9	.77	.81
11	Pr	7.1+	1.33	.063	.61	14	.77	1.25
10	Pr	38 +	1.35	.081	.63	17	.79	1.58
9	Pr	> 170 +	3.61	.097	1.85	7.7	1.87	.91
18	Pb	.097	1.11	.042	.34	15	.78	1.41
17	Pb	.331	1.40	.034	.85	13	.58	1.33
16	Pb	1.61	2.36	.041	1.61	11	.77	1.20
15	Pb	2.26	2.40	.047	1.71	9.1	.70	1.1
14	Pb	19.3	4.27	.087	3.07	4.9	1.25	.54
13	Pb	50.8	6.22	.1	4.5	3.0	2.7	.2
27	Ca	1	1.61	.038	.83	12	.88	.83
26	Ca	5	1.88	.059	1.13	8.0	.81	1.13
25	Ca	15	2.92	.074	1.34	10	1.63	1.34

+ denotes relative praseodymium concentration.

The addition of a small amount of foreign-impurity ions caused a large decrease in the rate of second-stage coloration. Then, as the concentration of the impurity ions was increased, the rate of second-stage coloration became larger. The minimum of a* for the four cations for which the impurity concentration was determined occurred at less than 1×10^{16} impurity ions per cc.

The suppression of the colorability caused by lead impurity which was observed by Sibley, Sonder, and Butler (52) occurred in a much later region of the coloration curve. They found that in this late stage of coloration, the larger the concentration of lead ions, the greater the suppression of coloration. However, this is probably not the same effect reported here since different regions of the coloration curve were studied.

Fröhlich and Altrichter (16) investigated the same region of the coloration curve that this work covered but they did not observe any suppression of the second-stage coloration rate for calcium-doped crystals. However, they observed that the rate of second-stage coloration increased with increasing calcium concentration. Their pure potassium chloride crystal was grown from reagent-grade material in an air atmosphere and therefore contained a large concentration of cation and oxygen-containing impurities. The concentration of impurities in their pure crystal was probably greater than the concentration necessary to reach the minimum in the second-stage coloration

rate. Thus, as they increased the concentration of calcium ions they would only observe an increase in a*.

Quantitative effect of impurities. No simple relationship was found between the total first-stage coloration, N_f^1, and the impurity concentration, N_o. Figure 20 shows a plot of the first-stage coloration against the impurity concentration for the four cations for which the impurity concentration was known. For lead and europium an equation of the form

$$N_f^1 = A\ N_o^b$$

is valid over the concentration range investigated. However, the constants A and b depend on the impurity present in the crystal. For lead and europium, the value of b is .26 and .51 and the value of A is 1.3×10^{12} and 1.2×10^{8} respectively, when N_f^1 and N_o are given in ions per cc.

Because the rate of coloration in the second stage reached its minimum at such a low concentration of impurity ions, no data was available from which to find a relationship between the suppression of a* and the impurity concentration. However, the following discussion will show that there is a correlation between a* and the impurity concentration after the minimum of a* is passed.

Table 13 lists the value of the ratio of the total first-stage coloration to the rate of coloration in the second stage.

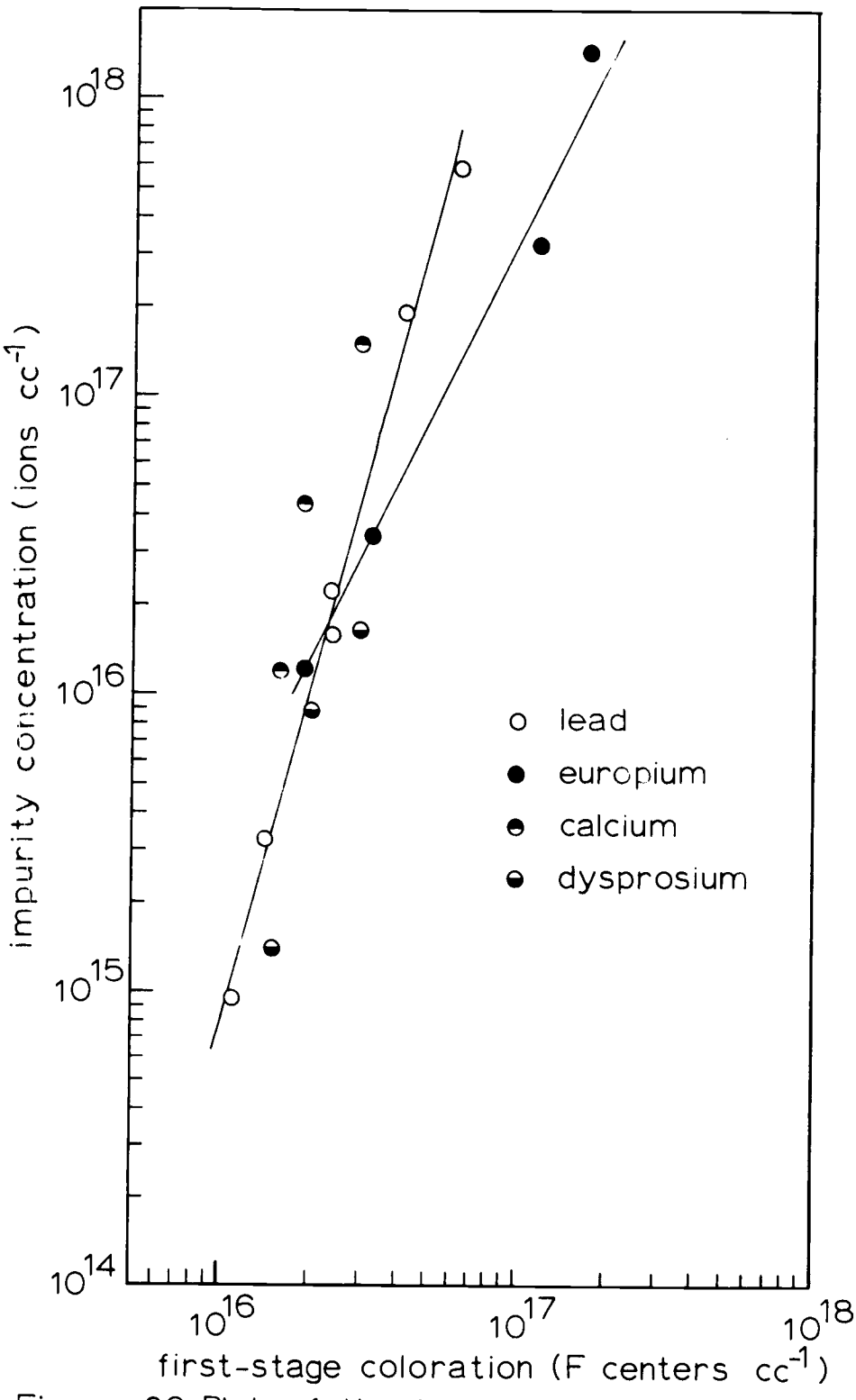

Figure 20. Plot of the impurity concentration against the total first-stage F-center coloration.

Table 13. Value of $\frac{N_f^1}{a^*}$ for the doped KCl crystals.

Sample	Impurity	Impurity Concentration (ions $cc^{-1} \times 10^{-16}$)	$\frac{N_f^1}{a^*}$ (hr^{-1})
8c	Eu	1.22	73
7c	Eu	3.40	87
6d	Eu	33	83
4d	Eu	147	80
18	Pb	.097	26
27	Pb	1.61	42
16	Pb	1.61	57
15	Pb	2.26	51
14	Pb	19.3	49
13	Pb	50.8	62
27	Ca	1	42
26	Ca	5	32
25	Ca	15	39
1d	Dy	.14	34
2d	Dy	.90	56
3d	Dy	1.68	48
12	Pr	1.0†	22
11	Pr	7.1†	21
10	Pr	38 †	17
9	Pr	>170 †	37
melt-grown pure	--	---	13

†Dontes relative Pr concentration.

It is observed that the ratio $\frac{N_f^1}{a^*}$ changes rapidly from its value of 13 for the pure crystal to a larger, constant number as the concentration of impurity is increased. The constant ratio is obtained after the minimum of a^* is reached. The transition of the ratio from the value obtained for the pure crystal to the constant value occurs at doping levels below approximately 1×10^{16} impurity ions per cc, which is in the concentration range where N_f^1 is remaining nearly constant and a^* is decreasing with increasing impurity-ion concentration. The constant value obtained in the doping region where a^* is increasing indicates that in this region the rate of second-stage coloration has the same functional dependance on the impurity concentration as the total first-stage coloration. However, the magnitude of the constant value obtained for $\frac{N_f^1}{a^*}$ depended on the impurity present in the crystal.

Effect of impurities on the second stage. According to the Pooley mechanism (38, 39), the effect of electron-trapping impurities would be to decrease the rate of coloration. As the concentration of the electron-trapping impurities becomes larger, the suppression of the rate of coloration should increase. This was varified by the results of Sibley et al. (52), who showed that as the lead-ion concentration in potassium chloride is increased, the rate of coloration in the later stages is suppressed.

The work reported here showed that during the second stage of coloration, the rate of second-stage coloration initially decreased to a minimum value with the addition of a small amount of impurity and then increased as the impurity concentration was further increased. The Pooley mechanism cannot account for an increase in the second-stage coloration rate. If the initial decrease in the rate of second-stage coloration is caused by the Pooley mechanism, it would be necessary to assume that a different process dominates the F-center growth at larger impurity concentrations causing the coloration rate to increase.

However, it is more probable that the Pooley mechanism is not the dominant process during the second stage of coloration, and only becomes a dominant factor during the very late stages of coloration.

Coloration of Pure KCl Crystals

Results

Solution-grown crystals. Three series of solution-grown crystals were prepared, two by the convection method and one by evaporation. It was observed that the colorability depended on the thickness of the crystal samples. Figure 21 shows the coloration curves of several samples taken from the first series of crystals

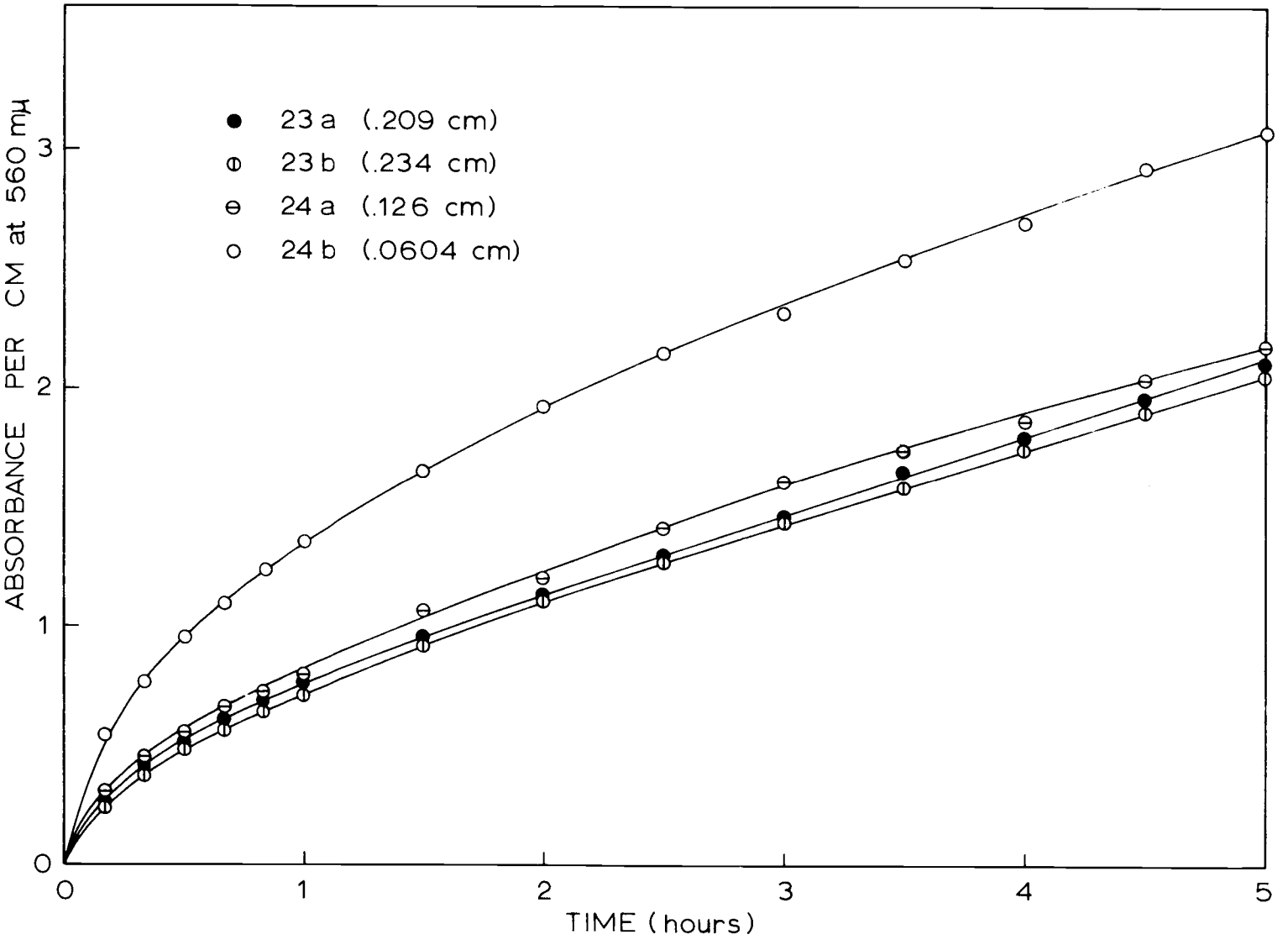

Figure 21. Coloration curves for solution-grown crystals of various thicknesses.

grown by convection and indicates that as the thickness of the samples is increased, the colorability decreases. This effect is probably caused by strain introduced into the crystal sample when it is cleaved from the original crystal block. Mechanical straining of a crystal is known to increase the colorability (78, p. 188-190). The thinner a crystal is cleaved, the more strain is introduced; therefore the thin crystal should color at a greater rate. The coloration curves were reproducible if the crystals were over two mm thick, therefore all coloration experiments were done on crystals of at least this size. It is interesting to note that the melt-grown crystals did not show this effect, indicating that they are either not as easily strained as the solution-grown crystals or their colorability is not as sensitive to the effect of strain.

Figure 22 shows the coloration curves for crystals grown in the several series. The colorability of crystals within a given series was reproducible to within five percent; however large differences existed between crystals grown in the different series. In Figure 22, sample 23b is from the first series grown by convection, samples 21 and 22 are from the second series grown by convection, and samples 19 and 20 were grown by evaporation. The difference in colorability of the KCl crystals grown in the different series could be caused by slightly different purity levels or a difference in the mechanical properties of the crystals.

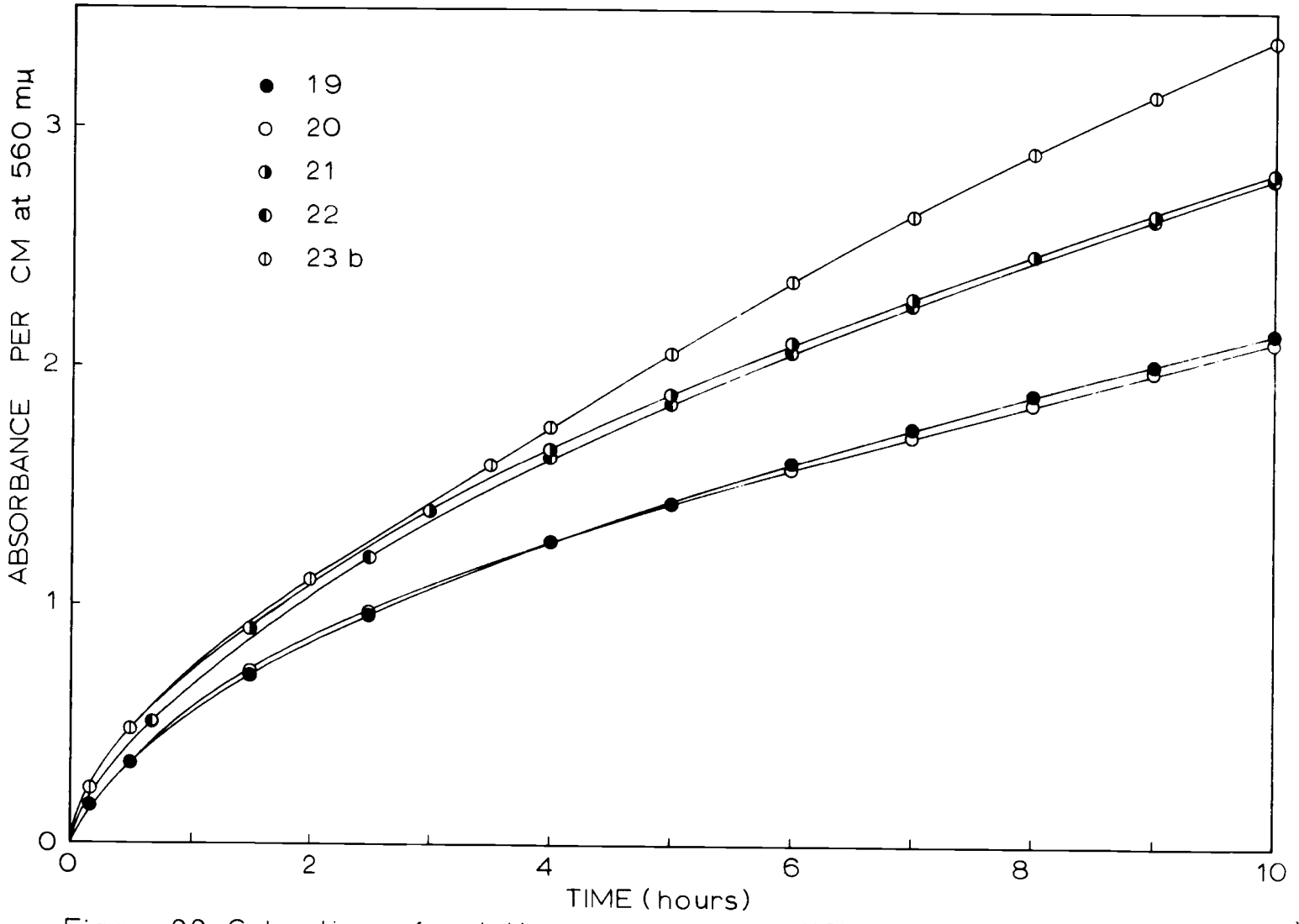

Figure 22. Coloration of solution-grown pure KCl crystals.

Hydroxide ions, present in a crystal, will affect the colorability of the crystal as shown by the work of Etzel and Allard (13). In order to determine if the crystals grown from solution are affected by the hydroxide impurity, some crystals were grown from a solution which was acidified with HCl. The coloration curves of sample 19, which was grown from a solution with a pH of 3, and sample 20, which was grown from a neutral solution, are shown in Figure 22. No significant difference exists between these two coloration curves, indicating that the concentration of hydroxide ion in the crystals is too low to affect the colorability.

Melt-grown crystals. The colorability of several pure crystals obtained from different sources was examined. Since all crystals contain some trace contamination, "pure" refers to crystals which have not been intentionally doped with impurities.

The Harshaw sample was obtained from the Harshaw Chemical Company and is a commercially available product. The Vinor crystal was obtained from the Vinor Laboratories and was grown in a vacuum employing HCl-treated zone-refined potassium chloride. The Anderson crystal was grown in our laboratory with the same system and procedure that has been described in Section II. The salt for this crystal was obtained from the Anderson Chemical Company and it was purified by vacuum distillation and chlorine treatment.

Figure 23 shows the coloration curves for these crystals and

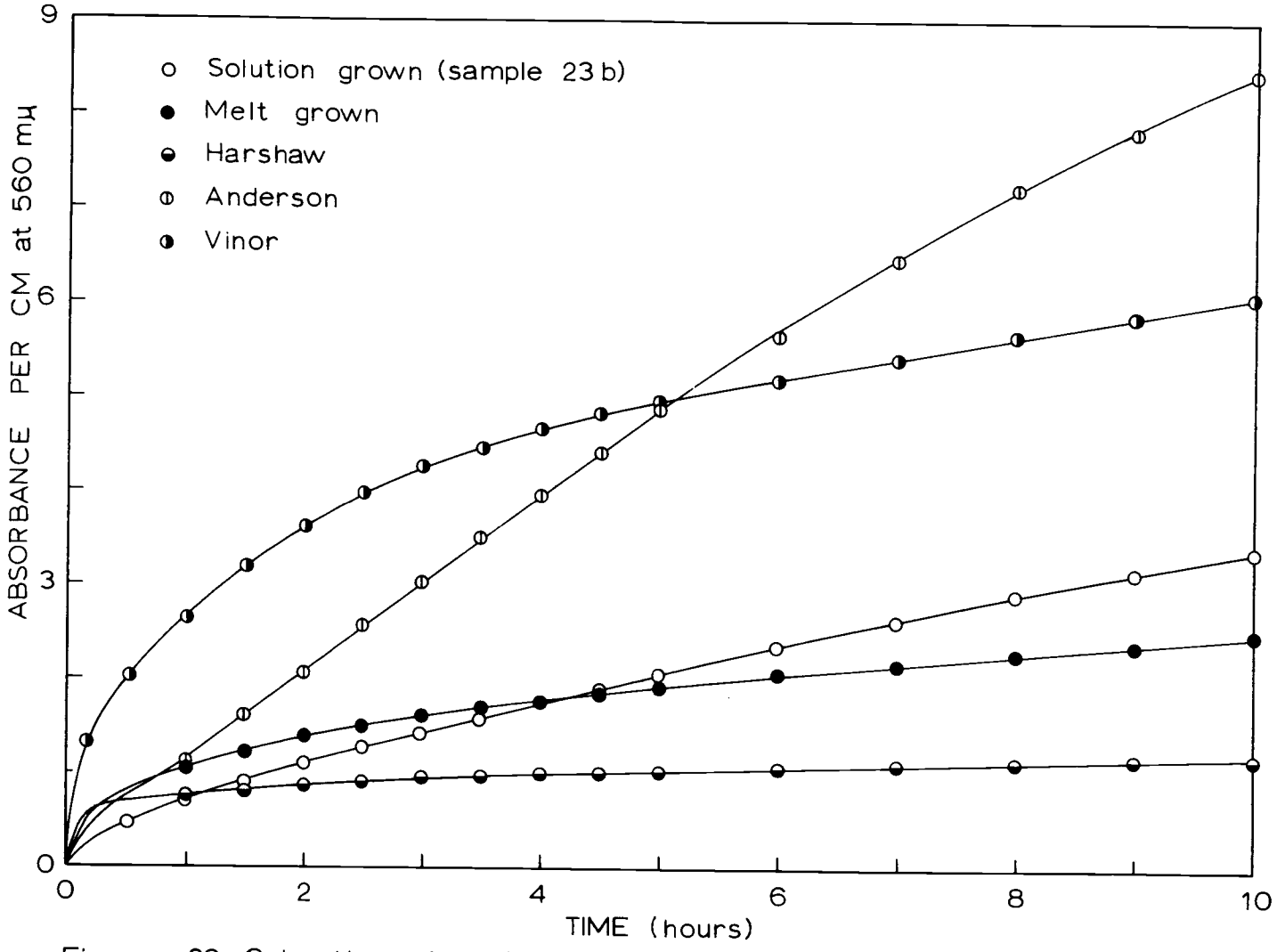

Figure 23. Coloration of various pure KCl crystals.

the first-stage coloration is shown in greater detail in Figure 24. The colorability is extremely sensitive to trace impurities and variations in the coloration curves of different KCl crystals has been reported by several authors (50, 54). Butler, Sibley, and Sonder (5) have observed that the late-stage coloration curves vary by as much a factor of four between samples of Harshaw KCl removed from different ingots.

Optical bleaching of the pure KCl crystals. Optical bleaching of the F center occurs if the crystal is exposed to light absorbed by the F center. The destruction of the F center by the photons occurs either by electron-hole recombination or by aggregation of the F centers to more complex electron-trapped centers. The rate of optical bleaching of the F center is very sensitive to the presence of impurities or mechanical strain in the crystal. Impurities or strain will increase the rate of optical bleaching.

Optical bleaching of the various pure crystals was done by exposing the crystals to light having a wavelength of 560 mμ from a Beckman Model DU spectrophotometer. The slit-width of the spectrophotometer was two mm and the tungsten light-source of the spectrophotometer was employed. Optical bleaching was done after the coloration experiment was concluded and the temperature of the crystal was controlled at 25° C.

Figure 25 shows the bleaching curves of the various pure

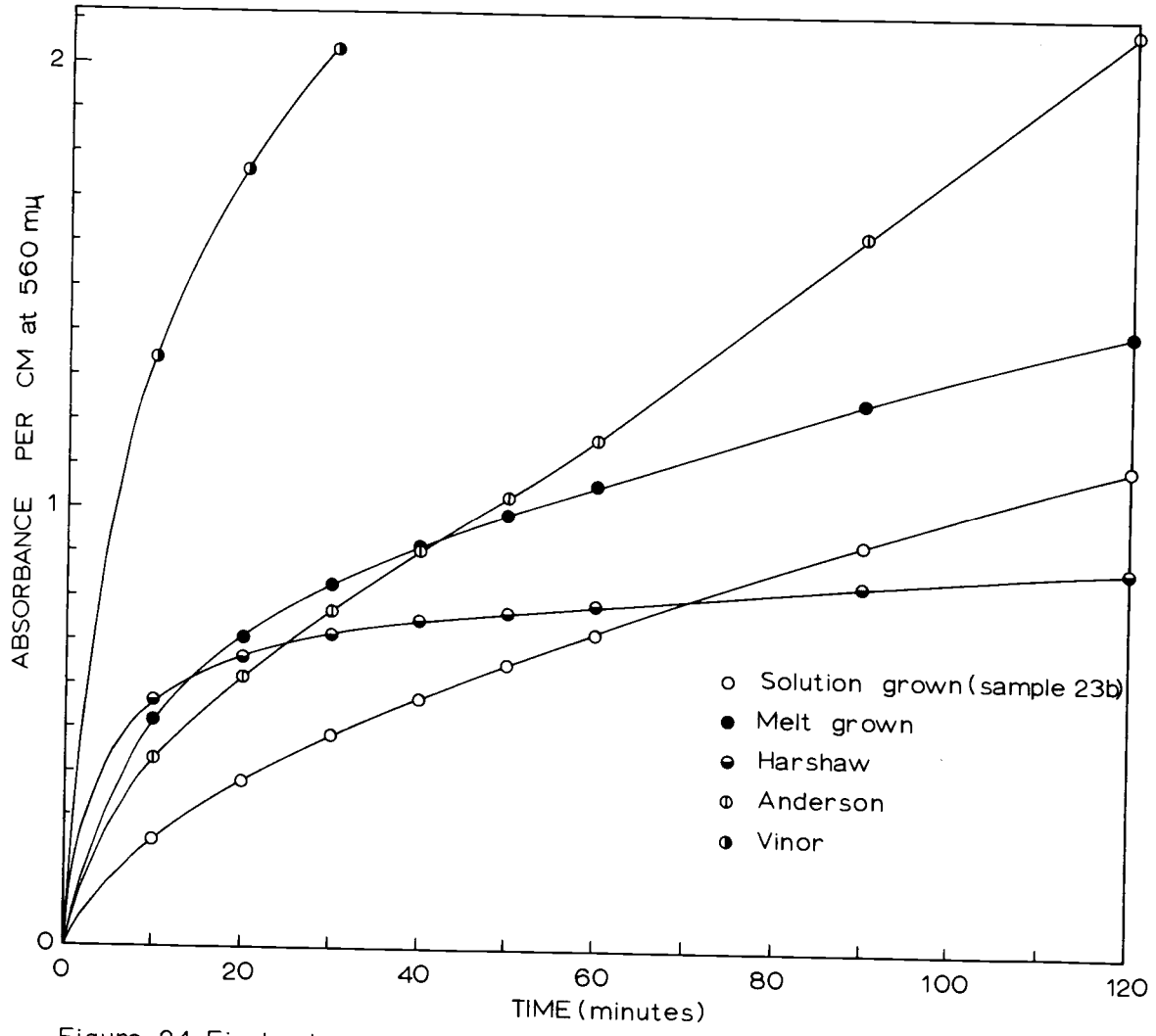

Figure 24. First-stage coloration of various pure KCl crystals.

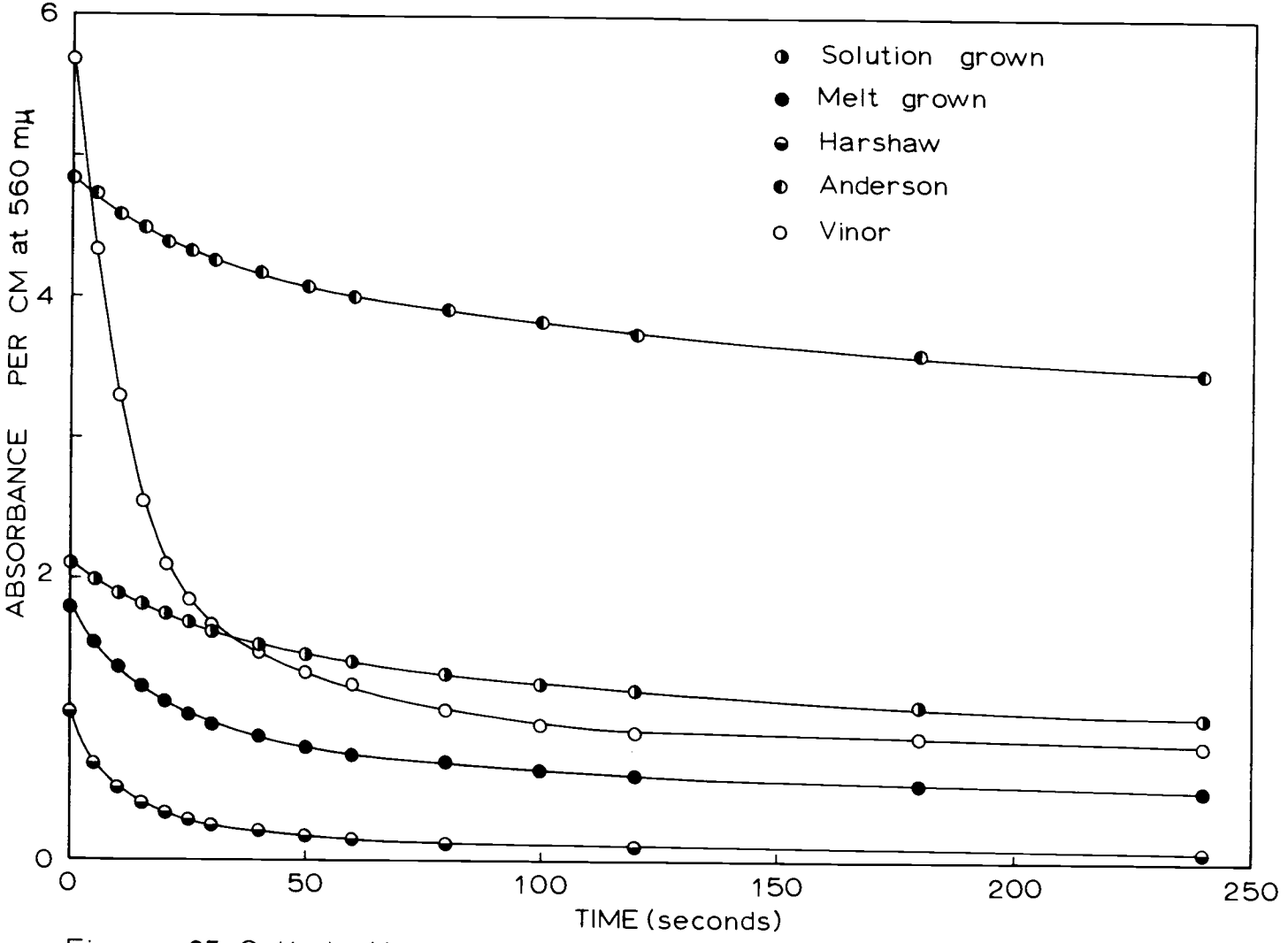

Figure 25. Optical bleaching of various pure KCl crystals.

samples. Since each crystal initially contained a different F-center concentration, the bleaching curves were normalized to the same initial F-center concentration. The normalized curves are shown in Figure 26. The large differences observed in the coloration curves are also apparent in the bleaching curves.

Analysis of coloration curves. The growth curves were fitted to the Mitchell, Wiegand, and Smoluchowski equation (31) and the values of the parameters which were determined are shown in Table 14.

Only the melt-grown crystal and the Harshaw crystal could be fitted to the equation over the entire irradiation period. The coloration curve for the Anderson crystal was linear over the first five hours of the irradiation, although the extrapolation of the linear region to the origin did not pass through zero. After five hours of irradiation the coloration rate began to decrease causing the coloration curve to become nonlinear. Because of the small first-stage coloration, the coloration curve for this crystal could not be fitted to the Mitchell, Wiegand, and Smoluchowski equation. The second-stage coloration rate, a*, was taken as the slope of the coloration curve during the linear region and the total first-stage coloration was taken as the intercept of the extrapolation of the linear region to the origin.

The solution-grown crystals grown by convection in the first series exhibited a linear region between two and six hours of

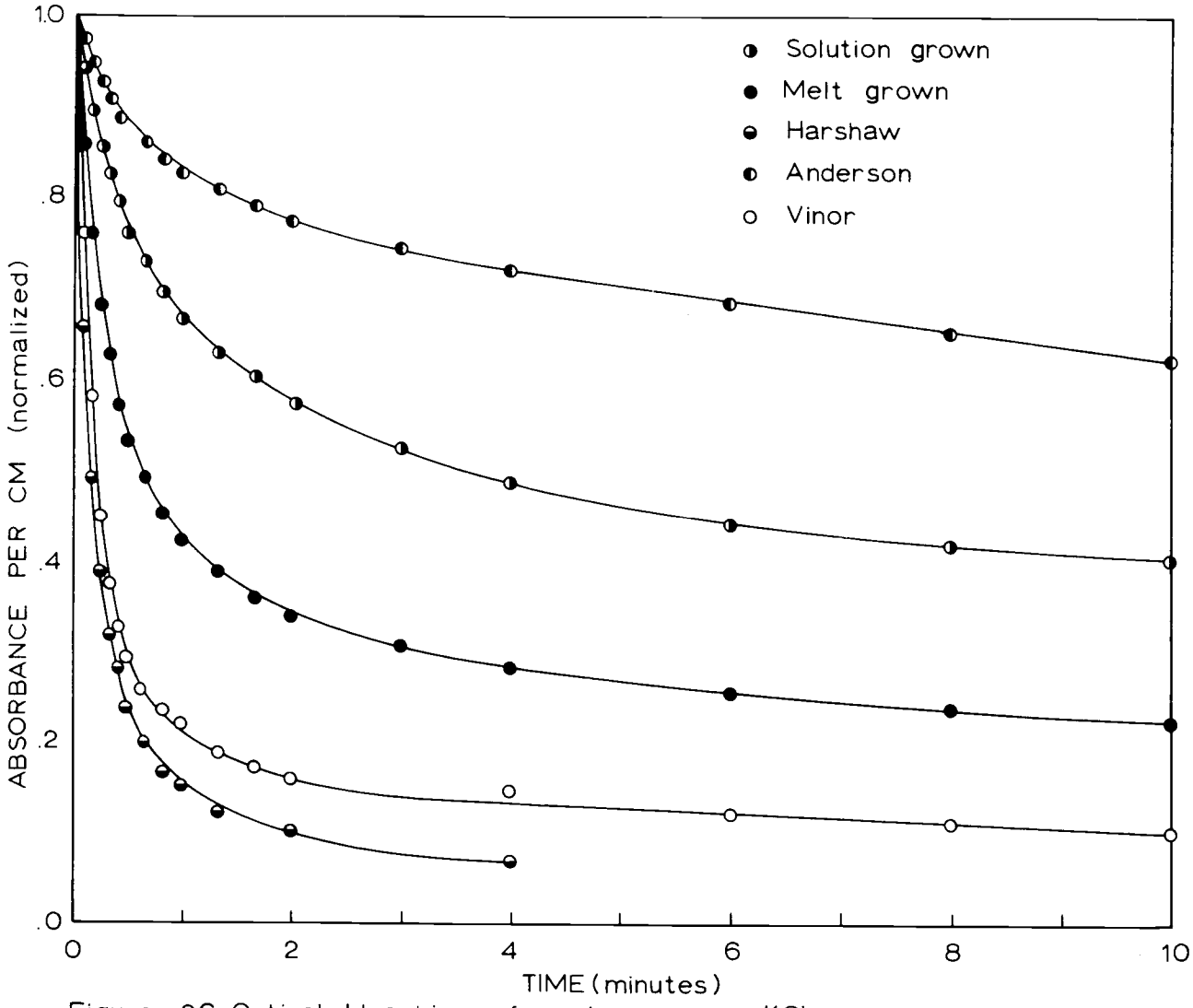

Figure 26. Optical bleaching of various pure KCl crystals.

Table 14. Curve fit for the various pure KCl crystals.

Crystal	First-stage Coloration (F-centers $cc^{-1} \times 10^{-16}$)	$a^* \times 10^{-16}$ (F-centers $cc^{-1} hr^{-1}$)	$n_o^* \times 10^{-16}$ (F-centers cc^{-1})	b^* (hr^{-1})	$n_o' \times 10^{-16}$ (F-centers cc^{-1})	c^* (hr^{-1})
Anderson	.22	.902	--	--	--	--
Solution-grown						
23 b	.53	.293	.20	7.2	.66	.20
20	.97	.159	.17	8	1.37	.40
Melt-grown	1.38	.104	.50	8.9	1.1	.50
Harshaw	.94	.021	.61	11	.39	.61

irradiation. For longer irradiation times, the rate of coloration decreased and the coloration curves became nonlinear. These crystals, such as sample 23b, could only be fitted over the first six hours of irradiation.

The other two series of solution-grown crystals did not exhibit any linear region over the irradiation period employed. However, the coloration curves could be fitted to the Mitchell, Wiegand, and Smoluchowski equation as shown by sample 20 listed in Table 14. The nonlinearity of solution-grown KCl (35) and NaCl (12, 41) has previously been reported.

Purity of the various crystals. It would be desirable to know the concentration of all the trace impurities in the pure crystals, for then it might be possible to explain the different colorabilities observed for the various pure crystals. Unfortunately, no method exists for measuring many of the impurities at concentrations below one ppm. Generally, several different methods are employed, each method being sensitive to several trace impurities and then from this data the overall purity of the crystal is estimated.

Sodium, rubidium, and bromine concentrations were determined for the various pure samples by neutron-activation analysis. The samples, approximately one gram, were irradiated for six hours in the rotating rack of a Triga Mark II reactor, and then counted at various intervals after the irradiation on a Nuclear Data 2200 System

4096 channel analyzer equipped with an Ortec 6 cm^2 lithium drifted germanium detector. No chemical separations were done. Table 15 lists the isotopes and the gamma-ray energy of the photopeaks employed for the determination of each element and Table 16 gives the results. Only the relative concentration is given for rubidium and bromine since standards were not used for these two elements. It should be noted that these impurities affect the colorability only at very large concentrations (2).

Table 15. Isotope properties for Na, Rb, and Br analysis.

Element	Isotope	Half-Life	Photopeak (Mev)
Sodium	^{24}Na	15 hrs	2.75 and 1.73
Rubidium	^{86}Rb	18.7 days	1.077
Bromine	^{82}Br	36 hrs	.554

Table 16. Concentration of Na, Rb, and Br in pure KCl.

Sample	Na (ppm)	Rb (relative)	Br (relative)
Harshaw	<1	1.0	1.00
Anderson	4.8±.7	19	.18
Melt-grown	1.6±.4	7	1.32
Solution-grown	<1	.9	.63
Solution*	5.0±.7	8	1.05

*This is KCl solution removed directly from the ion-exchange column after purification.

The electrical conductivity can be employed to estimate the total divalent-ion concentration in the crystals. The equation

$$N_o = 2.4 \times 10^{\left[23 - \frac{5700}{T_k}\right]}$$

given by Seevers (49, p. 22) was used to determine the total divalent-cation concentration, N_o, in ions per cc from the knee temperature, T_k, in °K. The knee temperature is the temperature at which the transition between extrinsic and intrinsic conductivity occurs. Seevers (49, p. 46) has reported the knee temperatures for all of the pure crystals listed in Table 17 except for the solution-grown crystal. The conductivity of the solution-grown crystal was measured by Schuerman (47). Table 17 gives the estimated divalent-ion concentrations of the various pure crystals.

Table 17. Estimate of the total divalent-cation content of the pure crystals.

Crystal	Knee Temperature (° K)	Impurity Concentration (ions per cc)
Solution-grown	539	3.6×10^{12}
Melt-grown	625	1.8×10^{14}
Harshaw	702	1.8×10^{15}
Anderson	714	2.4×10^{15}
Vinor	763	7.9×10^{15}

Several elements in Harshaw and Anderson crystals have been measured by Noble and Markham (34) employing semiquantitative spectrographic analysis. They reported that both of these crystals contained 100 ppm of calcium. However, their results for the Harshaw material are not in agreement with the neutron-activation analysis results reported by Anderson, Wiley, and Hendricks (1). These authors stated that Harshaw crystals contained only .1 ppm of calcium and for several other impurities their results are lower by a factor of ten from the results of Noble and Markham.

Coloration of annealed solution-grown crystals. The coloration of a melt-grown and a solution-grown crystal is shown in Figure 27 before and after heat treating the crystals. The crystals were annealed in the same system and at the same time to insure that both crystals received the same treatment. The annealing was done at 600° C for one week under an atmosphere of chlorine as described previously in Section II.

After annealing, it was observed that the two crystals colored in very nearly the same manner. At the present time the reason for the apparent similarity of the coloration curves is not known.

Discussion

Colorability as a criterion of purity. Several authors have suggested that the coloration during the first stage may be used as an

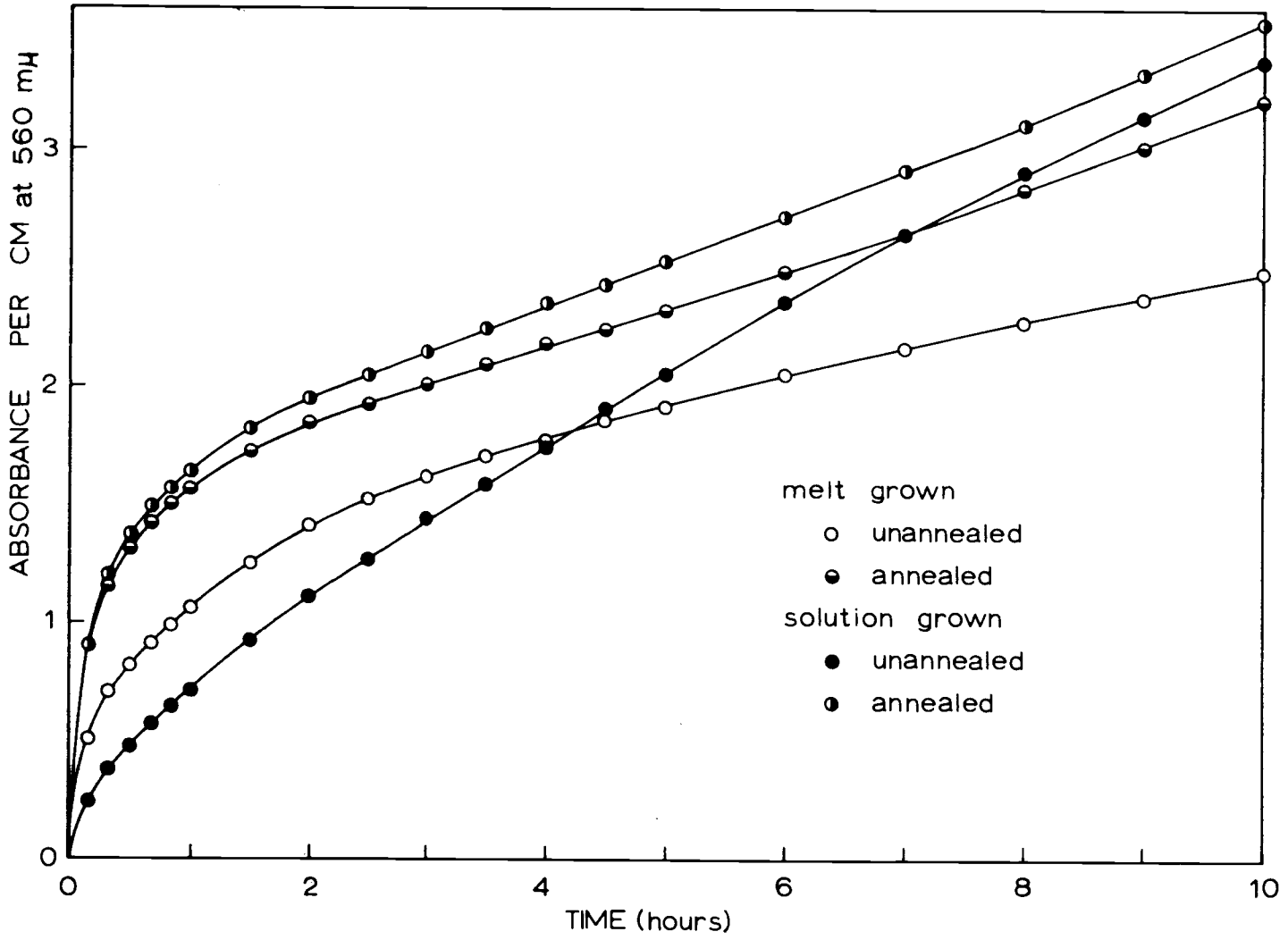

Figure 27. Coloration of annealed KCl crystals.

indication of purity. Since impurities increase the first stage of coloration at room temperature, and at low temperatures where impurities have little affect on the colorability there is almost no first stage; the first-stage coloration is probably not an intrinsic property of the crystal. Therefore, a relatively small first stage should be indicative of a relatively pure crystal.

While the colorability during the first stage did vary for the pure crystals studied, the coloration in the second stage differed by a much larger degree. The study of the coloration of the doped crystals showed that the presence of impurities suppressed the rate of coloration in the second stage if the impurity concentration was below approximately 1×10^{16} ions per cc. If we can assume that the pure crystals have impurity concentrations less than the amount necessary to reach the minimum in the rate of second-stage coloration, a large second-stage rate of coloration will indicate purity.

Therefore, a pure crystal should exhibit a small first-stage coloration and a large second-stage rate of coloration. The ratio $\frac{N_f^1}{a^*}$ will then be smallest for the most pure crystal. Table 18 lists this ratio for the pure crystals.

An examination of the coloration curves shown previously in Figure 23 shows that the Vinor crystal has a much larger first-stage coloration than the other pure crystals. However, the ratio $\frac{N_f^1}{a^*}$

Table 18. Ratio of N_f^1 to a* for the pure crystals.

Sample	$\frac{N_f^1}{a^*}$ (hr^{-1})
Anderson	.24
Solution-grown	
23b	1.8
20	6.1
Melt-grown	13
Vinor	17
Harshaw	45

for the Vinor crystal is almost the same as the melt-grown crystal which, if the above argument is valid, indicates a comparable purity level. But the presence of the large first-stage coloration indicates that the crystal is not pure and the small value of the ratio may result from the incorporation of an impurity which has little effect on the ratio. Seevers (49, p. 46-51) has shown that the Vinor crystal contains large amounts of oxygen-containing impurities, such as OH^- and O_2^-, and this probably results in the large initial colorability. This crystal will not be considered as pure in the following discussion.

For the other crystals, the order of decreasing purity according to the above criterion would be Anderson, solution-grown, melt-grown, and Harshaw. It should also be observed that the ease of

optical bleaching increased in the same order. This indicates the stability of the F center to optical bleaching was largest in the Anderson crystal and smallest in the Harshaw crystal. Since impurities will increase the ease of optical bleaching, this also indicates that the purity varies in the above order. The stability of the F center in the various pure crystals with respect to thermal bleaching at 25° C follows the same order. The crystals were kept in the dark after the gamma irradiation and the decrease of the F-center concentration was measured. The concentration of F centers in Harshaw KCl decreased by 13 percent during a 59 hour period after the irradiation, while the Anderson crystal showed no measurable decrease in the F-center concentration 58 hours after the irradiation.

The order of purity for the various crystals determined from the colorability is the same as the purity order determined from conductivity measurements except for the Anderson crystal. The coloration of this crystal indicated that it had the highest purity, while the conductivity data indicated that it was less pure than the Harshaw crystal. However, the impurities which affected these two properties are probably not the same. Srinivasan and Compton (56) have shown that zone refining of KCl will decrease the knee temperature of the conductivity but had no effect on the colorability. Therefore, the Anderson crystal may be very low in the type of impurities which affected the colorability, but contains a large concentration of impurities

of the type which affected the ionic conductivity.

Coloration of Calcium-Doped Solution-Grown Crystals

In order to determine the effect of impurities on the colorability of solution-grown crystals, several crystals were grown from solutions containing calcium ions. Figure 28 shows the coloration curves of these crystals and Table 19 gives the calcium-ion concentration in the solutions. At 25° C each bottle contained 220 ml of saturated KCl solution to which a given quantity of reagent-grade $CaCl_2 \cdot 2H_2O$ was added. The molarity of the calcium in the solution is calculated at 25° C.

Table 19. Calcium concentration in solutions from which crystals were grown.

Sample	Grams $CaCl_2 \cdot 2H_2O$ in Solution	Ca^{++} Concentration (mole $liter^{-1}$)
28	13.3	.41
29	1.92	.059
30	1.08	.033
31	.51	.016

The coloration curve for the pure crystal to which the calcium-doped crystals are compared in Figure 28 is the average of the coloration curves for samples 20 and 21 shown previously in Figure 22.

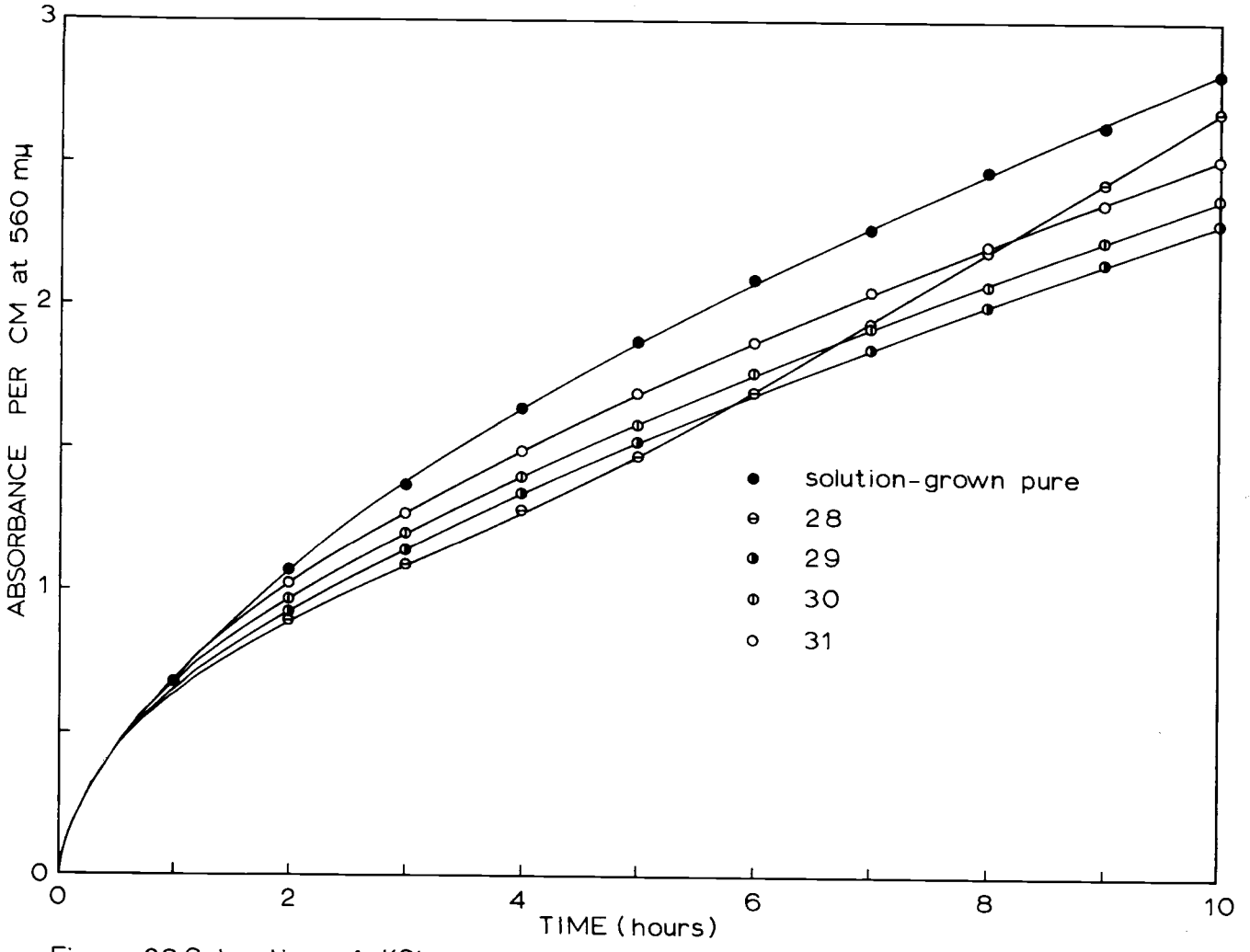

Figure 28.Coloration of KCl crystals grown from aqueous solutions containing calcium.

These pure crystals and the calcium-doped crystals were grown in the same series which was the second series grown by convection.

The coloration during the first stage is not changed significantly in these crystals, however the rate of coloration in the second stage is suppressed. The larger the concentration of calcium in the solution, the greater the suppression of the rate of coloration in the second stage. However, sample 28 which was grown from the solution containing the largest calcium concentration exhibited an inflection point not observed in the other crystals.

The differences observed in the coloration curves for the solution-grown calcium-doped crystals are larger than the experimental error. Figure 29 shows the coloration of three crystals removed from the solution which contained the largest concentration of calcium and shows that the coloration curves agree within five percent. The coloration curve for sample 28 shown previously in Figure 28 was the average of these three coloration curves.

If the effect of impurities on the solution-grown crystals is the same as on the melt-grown crystals, it would appear that we are in the region of very low impurity concentrations where the first stage is unaffected but the rate of second-stage coloration is decreasing with increasing impurity concentration. It was observed that for the calcium-doped melt-grown crystals the minimum of the second-stage coloration rate occurred at less than 1×10^{16} calcium ions per cc.

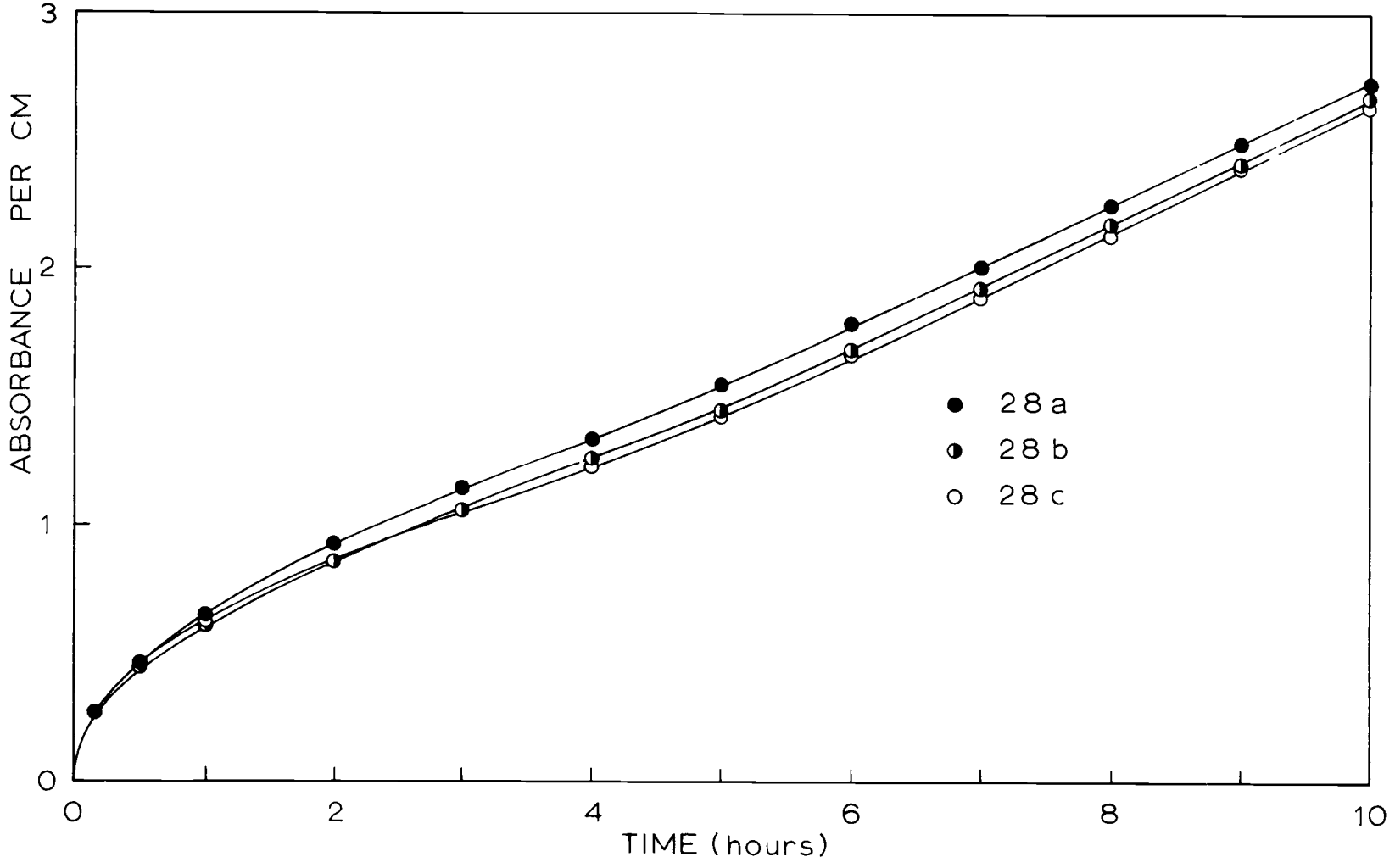

Figure 29. Coloration of three KCl crystals removed from same calcium-doped solution.

Thus, the concentration of calcium in these calcium-doped solution-grown crystals is probably less than 1×10^{16} ions per cc.

Employing this value as the upper limit for the calcium concentration, an upper limit can be calculated for the distribution coefficient of calcium between the solution and the crystal. The distribution coefficient, D, is

$$D = \frac{N_c}{M}$$

where N_c and M are the concentration of calcium in the crystal and the solution, respectively. The units of D will be ions liter cc^{-1} $mole^{-1}$ if N_c is reported in ions per cc and M is the molarity. The most concentrated calcium solution was .41 molar and if the calcium-ion concentration of the crystal grown from this solution was less than 1×10^{16} ions per cc, the upper limit for the distribution coefficient will be 2×10^{16} ions liter cc^{-1} $mole^{-1}$.

BIBLIOGRAPHY

1. Anderson, S., J. S. Wiley and L. J. Hendricks. Zone refining and chemical analysis of KCl and KBr. Journal of Chemical Physics 32:949-950. 1960.

2. Arends, J., H. W. den Hartog and A. C. Dekker. F-center formation in mixed crystals of alkali halides. Physica Status Solidi 10:105-112. 1965.

3. Asundi, R. K. and R. C. Naik. On the absorption and fluorescence spectra of praseodymium doped KCl single crystal. Current Science (India) 34:550-552. 1965.

4. Botsaris, G. D., B. A. Mason and R. C. Reid. Growth of potassium chloride crystals from aqueous solutions. II. Growth in a gamma-radiation field. Journal of Chemical Physics 46:192-198. 1967.

5. Butler, C. T., W. A. Sibley and E. Sonder. Variation of coloration rates and luminescence in Harshaw potassium chloride. Journal of Chemical Physics 39:242-243. 1963.

6. Chadderton, L. T., D. V. Morgan and I. McC. Torrens. Computer simulation of the Varley mechanism. Physics Letters (London) 20:329-331. 1966.

7. Cook, J. Dislocation etching solution for potassium chloride and other alkali halides. Journal of Applied Physics 32:2492. 1961.

8. Crawford, J. H. and C. M. Nelson. Defect interactions in irradiated calcium-doped potassium chloride. Physical Review Letters 5:314-315. 1960.

9. Crowe, G. J., W. Fuchs and D. A. Wiegand. Schottky disorder and lattice relaxation in single crystals of NaCl due to x-irradiation at room temperature. Physical Review Letters 16: 1154-1155. 1966.

10. Dexter, D. L. Absorption of light by atoms in solids. Physical Review 101:48-55. 1956.

11. Dexter, D. L. Varley mechanism for defect formation in alkali halides. Physical Review 118:934-935. 1960.

12. Dolgopolova, A. V., L. V. Kovaleva, S. A. Sazonova and B. S. Skorobogatov. On the luminescence of rare earth ions in NaCl crystals. Optics and Spectroscopy 17:73. 1964.

13. Etzel, H. W. and J. G. Allard. Color center formation in sodium chloride. Physical Review Letters 2:452-454. 1959.

14. Fredericks, W. J., F. E. Rosztoczy and J. Hatchett. Investigation of crystal growth processes. Palo Alto, 1963. 24 numb. leaves. (Stanford Research Institute. Final Report. SRI Project no. PAU-3523. Results presented at 1962 International Color Center Symposium, Stuttgart, Germany)

15. Fredericks, W. J., L. W. Schuerman and L. C. Lewis. An investigation of crystal growth processes. Corvallis, 1967. 45 numb. leaves. (Oregon State University. Final Report. Grant no. AF-AFOSR 217-63, Project Task:9762-02)

16. Fröhlich, F. and S. Altrichter. Über die Verfärbung von reinen und Ca-dotierten KCl-und NaCl-Kristallen unter der Einwirkung von γ-Strahlung. Annalen der Physik 17:143-159. 1966.

17. Gordon, R. B. and A. S. Nowick. Structure sensitivity of the x-ray coloration of NaCl crystals. Physical Review 101:977-983. 1956.

18. Gruzensky, Paul M. Growth of large sodium chloride crystals from solution for color-center studies. Journal of Chemical Physics 43:3807-3810. 1965.

19. Hersh, H. N. Formation of color centers in alkali halides using nonionizing (exciton) radiation. Bulletin of the American Physical Society 10:582. 1965.

20. Hills, Marian E. and Allen B. Scott. Incorporation of trivalent cations in crystalline potassium chloride. Nature 192:1066-1067. 1961.

21. Holmes, Robert Edward. Electrical and optical properties of potassium chloride single crystals containing lead ion. Ph. D. thesis. Corvallis, Oregon State University, 1966. 191 numb. leaves.

22. Howard, R. E. and R. Smoluchowski. Formation of interstitials in alkali halides by ionizing radiation. Physical Review 116: 314-315. 1959.

23. Howard, R. E., Seymour Vosko and R. Smoluchowski. Mechanism for production of interestitials in KCl by x rays at low temperatures. Physical Review 122:1406-1408. 1961.

24. Kaenzig, W. and T. O. Woodruff. Electron spin resonance of H centers. Physical Review 109:220-221. 1958.

25. Kelting, Heinke and Horst Witt. Über KCl-Kristalle mit Zusätzen von Erdalkalichloriden. Zeitschrift für Physik 126: 697-710. 1949.

26. Klick, Clifford C. Mechanism for coloration of alkali halides at low temperatures. Physical Review 120:760-762. 1960.

27. Klick, Clifford C. and David A. Patterson. Low-temperature coloration in KCl and KBr near the fundamental edge. Physical Review 130:2169-2176. 1963.

28. Konitzer, J. D. and J. J. Markham. Experimental study of the shape of the F-band absorption in KCl. Journal of Chemical Physics 32:843-856. 1960.

29. Lyon, William S. Jr. (ed.). Guide to activation analysis. Princeton, D. Van Nostrand, 1964. 179 p.

30. Mitchell, P. V., D. A. Wiegand and R. Smoluchowski. F-center growth curves. Physical Review 117:442-443. 1960.

31. _____. Formation of F centers in KCl by x rays. Physical Review 121:484-498. 1961.

32. Nadeau, J. S. Hardening of potassium chloride by color centers. Journal of Applied Physics 34:2248-2253. 1963.

33. _____. Radiation hardening in alkali halide crystals. Journal of Applied Physics 35:1248-1255. 1964.

34. Noble, G. A. and J. J. Markham. Effect of impurities on the F band in KCl. Journal of Chemical Physics 41:1880-1881. 1964.

35. Okamoto, Fuimo and Allen B. Scott. Formation and optical bleaching of F centers: impurity effects. Journal of the Physical Society of Japan, sup II, 18:243-249. 1963.

36. Peisl, H., R. Balzer and W. Waidelich. Schottky and Frenkel disorder in KCl with color centers. Physical Review Letters 17:1129-1131. 1966.

37. Pissarenko, V. F. and S. V. Voropaeva. The luminescence of Dy^{3+} in NaCl and KCl. Physica Status Solidi 15:K95-K96. 1966.

38. Pooley, D. F-center production in alkali halides by radiationless electron hole recombinations. Solid State Communications 3: 241-243. 1965.

39. _____. The inhibition of F-centre production in alkali halides caused by electron-trapping impurities. Proceedings of the Physical Society (London) 89:723-733. 1966.

40. Rabin, Herbert. X-ray expansion and coloration of undoped and impurity-doped NaCl crystals. Physical Review 116:1381-1389. 1959.

41. Rabin, Herbert and Clifford C. Klick. Formation of F centers at low and room temperatures. Physical Review 117:1005-1010. 1960.

42. Reisfeld, R. and A. Glasner. Absorption and fluorescence spectra of Eu^{2+} in alkali halide crystals. Journal of the Optical Society of America 54:331-333. 1964.

43. Ritz, Victor H. F-center production efficiencies at liquid-helium temperature. Physical Review 133:A1452-A1470. 1964.

44. _____. Vacancy-production efficiencies in KBr at low temperatures. Physical Review 142:505-513. 1966.

45. Rivas, J. L. Alvarez and P. W. Levy. X-ray-induced first-stage coloring of NaCl. Physical Review 162:816-823. 1967.

46. Röhrig, R. Electron spin resonance of Eu^{++} in alkali halides. Physics Letters 16:20-21. 1965.

47. Schuerman, L. W. Graduate Student, Oregon State University, Dept. of Chemistry. Personal communication. Corvallis, Oregon. 1968.

48. Schulman, James H. and W. Dale Compton. Color centers in solids. New York, Pergamon, 1962. 368 p.

49. Seevers, Robert Edward. Electrical conductivity of additively colored potassium chloride crystals. Ph. D. thesis. Corvallis, Oregon State University, 1968. 126 numb. leaves.

50. Sibley, W. A. and E. Sonder. F- and M-band absorption in heavily gamma-irradiated KCl. Physical Review 128:540-546. 1962.

51. _____. Hardening of KCl by electron and gamma irradiation. Journal of Applied Physics 34:2366-2370. 1963.

52. Sibley, W. A., E. Sonder and C. T. Butler. Effect of lead on the room-temperature colorability of KCl. Physical Review 136:A537-A541. 1964.

53. Smakula, A. Über Erregung und Entfärbung lichtelektrisch leitender Alkalihalogenide. Zeitschrift für Physik 59:603-614. 1930.

54. Sonder, E. Magnetism of KCl. Physical Review 125:1203-1208. 1962.

55. Sonder, E. and W. A. Sibley. Radiation equilibrium of F and M centers in KCl. Physical Review 129:1578-1582. 1963.

56. Srinivasan, T. M. and W. D. Compton. X-ray generation of color centers in zone-refined KCl and KBr. Physical Review 137:A264-A272. 1965.

57. Varley, J. H. O. A mechanism for the displacement of ions in an ionic lattice. Nature 174:886-887. 1954.

58. _____. A new interpretation of irradiation-induced phenomena in alkali halides. Journal of Nuclear Energy 1: 130-143. 1954.

59. Wagner, Max and W. E. Bron. Rare-earth ions in the alkali halides. II. Pseudolocalized vibrational frequencies. Physical Review 139:A223-A233. 1965.

60. Williams, Ferd E. Theory of defect formation in alkali halides by ionizing radiation. Physical Review 126:70-72. 1962.

61. Zahrt, John David. Thermodynamics of the reaction between F and M centers. M. S. thesis. Corvallis, Oregon State University, 1965. 45 numb. leaves.